

UNIVERSIDAD DE CONCEPCIÓN



CENTRO DE INVESTIGACIÓN EN
INGENIERÍA MATEMÁTICA (CI²MA)



A posteriori error analysis of a Banach spaces-based fully mixed
FEM for double-diffusive convection in a fluid-saturated porous
medium

SERGIO CAUCAO, GABRIEL N. GATICA,
JUAN P. ORTEGA

PREPRINT 2022-12

SERIE DE PRE-PUBLICACIONES

A posteriori error analysis of a Banach spaces-based fully mixed FEM for double-diffusive convection in a fluid-saturated porous medium*

SERGIO CAUCAO[†] GABRIEL N. GATICA[‡] JUAN P. ORTEGA[§]

Abstract

In this paper we consider a Banach spaces-based fully-mixed variational formulation that has been recently proposed for the coupling of the stationary Brinkman–Forchheimer and double-diffusion equations, and develop a reliable and efficient residual-based *a posteriori* error estimator for the 2D and 3D versions of the associated mixed finite element scheme. For the reliability analysis, we employ the strong monotonicity and inf-sup conditions of the operators involved, along with a suitable assumption on the data, stable Helmholtz decomposition in nonstandard Banach spaces, and local approximation properties of the Raviart–Thomas and Clément interpolants. In turn, inverse inequalities, the localization technique through bubble functions, and known results from previous works, are the main tools yielding the efficiency estimate. Finally, several numerical examples confirming the theoretical properties of the estimator and illustrating the performance of the associated adaptive algorithms, are reported. In particular, the case of flow through a 2D porous media with channel networks is considered.

Key words: Brinkman–Forchheimer equations, double-diffusion equations, fully-mixed finite element methods, Banach spaces, *a posteriori* error analysis, reliability, efficiency.

Mathematics subject classifications (2000): 65N30, 65N12, 65N15, 35Q79, 76R05, 76D07

1 Introduction

We have recently introduced and analyzed in [5] a Banach spaces-based fully-mixed variational formulation for the steady double-diffusive convection in a fluid-saturated porous medium described by the coupling of the stationary Brinkman–Forchheimer and double-diffusion equations in \mathbb{R}^n , $n \in \{2, 3\}$. In there, besides the velocity, temperature, and concentration, the approach introduces the velocity gradient, the pseudostress tensor, and a pair of vectors involving the temperature/concentration, its gradient and the velocity, as further unknowns. As a consequence, a new fully mixed variational formulation presenting a Banach spaces framework in each set of equations is obtained. In this way, and differently from the techniques previously developed for this and related coupled problems, no

*This work has been supported by ANID-Chile through the projects ACE 210010, CENTRO DE MODELAMIENTO MATEMÁTICO (FB210005), ANILLO OF COMPUTATIONAL MATHEMATICS FOR DESALINATION PROCESSES (ACT210087), project Fondecyt 11220393, and BECAS/DOCTORADO NACIONAL 21201539; and by Centro de Investigación en Ingeniería Matemática (CI²MA), Universidad de Concepción.

[†]Departamento de Matemática y Física Aplicadas, Universidad Católica de la Santísima Concepción, Casilla 297, Concepción, Chile, email: scaucao@ucsc.cl.

[‡]CI²MA and Departamento de Ingeniería Matemática, Universidad de Concepción, Casilla 160-C, Concepción, Chile, email: ggatica@ci2ma.udec.cl.

[§]CI²MA and Departamento de Ingeniería Matemática, Universidad de Concepción, Casilla 160-C, Concepción, Chile, email: jportega@ci2ma.udec.cl

augmentation procedure needs to be incorporated now into the formulation nor into the solvability analysis. The resulting non-augmented scheme is then written equivalently as a fixed-point equation, so that the well-known Banach theorem, combined with classical results on nonlinear monotone operators and Babuška-Brezzi's theory in Banach spaces, are applied to prove the unique solvability of the continuous and discrete systems. Appropriate finite element subspaces satisfying the required discrete inf-sup conditions as well as optimal *a priori* error estimates are specified in [5].

Now, it is well known that adaptive algorithm based on *a posteriori* error estimates are very well suited to recover the loss of orders of convergence of most of the standard Galerkin procedures, such as finite element and mixed finite element methods, that are applied, specially to nonlinear problems, under the eventual presence of singularities or high gradients of the exact solutions. In particular, this powerful tool has been applied to quasi-Newtonian fluid flows obeying the power law, which include the Brinkman–Forchheimer model. In this direction, we refer to [18], [16], [19], [30], and [9], for different contributions addressing this interesting issue. Particularly, in [18] an *a posteriori* error estimator defined via a non-linear projection of the residues of the variational equations for a three-field model of a generalized Stokes problem was proposed and analyzed. In turn, a new *a posteriori* error estimator for a mixed finite element approximation of non-Newtonian fluid flow problems is developed in [19]. We observe that this mixed formulation, as in the finite volume methods, possesses local conservation properties, namely conservation of the momentum and the mass. Later on, *a posteriori* error analyses for the aforementioned Brinkman–Darcy–Forchheimer model in velocity-pressure formulation have been developed in [30]. In fact, two types of error indicators related to the discretization and to the linearization of the problem are established. Furthermore, the first contribution devoted to derive an *a posteriori* error analysis of the primal-mixed finite element method for the Navier–Stokes/Darcy–Forchheimer coupled problem was proposed and analyzed in [9]. More precisely, usual techniques employed within the Hilbertian framework are extended in [9] to the case of Banach spaces by deriving a reliable and efficient *a posteriori* error estimator for the mixed finite element method introduced in [4]. The above includes corresponding local estimates and new Helmholtz decompositions for the reliability, as well as respective inverse inequalities and local estimates of bubble functions for the efficiency. Meanwhile, *a posteriori* error analysis of a momentum conservative Banach space-based mixed finite element method for the Navier–Stokes problem was developed in [3]. Standard arguments relying on duality techniques, a suitable Helmholtz decomposition in Banach frameworks and classical approximation properties, are combined there with corresponding small data assumptions to derive the reliability of the estimators. In turn, similar techniques to those in [3] are employed as well in [23] to derive reliable and efficient residual-based *a posteriori* error estimators in 2D and 3D for the fully-mixed finite element methods introduced in [12] and [13], thus providing the first *a posteriori* error analyses of non-augmented Banach spaces-based mixed finite element methods for the stationary Boussinesq and Oberbeck-Boussinesq systems. Finally, we refer to [10] for a recent *a posteriori* error analysis of the partially augmented mixed formulation for the coupled Brinkman–Forchheimer and double-diffusion equations introduced in [8]. We remark that *a posteriori* error analysis techniques developed in [24], [25], [14], [6], [7], and [15] for augmented-mixed formulations in Hilbert spaces, with the ones described in [9] and [3] for Banach spaces-based mixed formulations are combined in [10] to develop two reliable and efficient residual-based *a posteriori* error estimators in two and three dimensions.

According to the above discussion, and aiming to continue extending the knowledge on the numerical analysis of nonlinear and coupled problems, in this paper we proceed similarly to [3] and [23] and derive reliable and efficient residual-based *a posteriori* error estimators in 2D and 3D for the fully-mixed finite element method introduced in [5]. This means that our analysis begins by applying the strong monotonicity and inf-sup conditions of the operators defining the continuous formulation. Next,

we apply suitable Helmholtz decompositions in non-standard Banach spaces, local approximation properties of the Clément and Raviart–Thomas interpolants, and small data assumption, to prove the reliability of a residual-based estimator. In turn, the efficiency estimate is consequence of standard arguments such as inverse inequalities, the localization technique based on bubble functions, and other known results to be specified later on in Section 3.3. We remark that up to the authors’ knowledge, the present work provides the first *a posteriori* error analyses of non-augmented Banach spaces-based mixed finite element methods for the coupling of the stationary Brinkman–Forchheimer and double-diffusion equations.

The rest of this work is organized as follows. The remainder of this section introduces some standard notations and functional spaces. In Section 2 we recall from [5], the model problem and its continuous and discrete fully-mixed variational formulations. Next, in Section 3 we derive in full details a reliable and efficient residual-based *a posteriori* error estimator for the 2D version of the problem. This includes preliminary results to be utilized for the derivation of the reliability and efficiency estimates, and then the proofs of the latter themselves, respectively. Then, in Section 4 we establish the 3D version of the *a posteriori* error estimator provided in Section 3. Finally, several numerical results confirming the reliability and efficiency of the *a posteriori* error estimator, as well as the good performance of the associated adaptive algorithm, and confirming the recovery of optimal rates of convergence, are reported in Section 5.

1.1 Preliminary notations

Let us denote by $\Omega \subset \mathbb{R}^n, n \in \{2, 3\}$, a given bounded domain with polyhedral boundary Γ , and let \mathbf{n} be the outward unit normal vector on Γ . Standard notation will be adopted for Lebesgue spaces $L^p(\Omega)$ and Sobolev spaces $W^{s,p}(\Omega)$, with $s \in \mathbb{R}$ and $p > 1$, whose corresponding norms, either for the scalar, vectorial, or tensorial case, are denoted by $\|\cdot\|_{0,p;\Omega}$ and $\|\cdot\|_{s,p;\Omega}$, respectively. In particular, given a non-negative integer m , $W^{m,2}(\Omega)$ is also denoted by $H^m(\Omega)$, and the notations of its norm and seminorm are simplified to $\|\cdot\|_{m,\Omega}$ and $|\cdot|_{m,\Omega}$, respectively. By \mathbf{M} and \mathbb{M} we will denote the corresponding vectorial and tensorial counterparts of the generic scalar functional space M , and $\|\cdot\|$, with no subscripts, will stand for the natural norm of either an element or an operator in any product functional space. In turn, for any vector field $\mathbf{v} = (v_i)_{i=1,n}$, we let $\nabla \mathbf{v}$ and $\operatorname{div}(\mathbf{v})$ be its gradient and divergence, respectively. Furthermore, for any tensor fields $\boldsymbol{\tau} = (\tau_{ij})_{i,j=1,n}$ and $\boldsymbol{\zeta} = (\zeta_{ij})_{i,j=1,n}$, we let $\mathbf{div}(\boldsymbol{\tau})$ be the divergence operator div acting along the rows of $\boldsymbol{\tau}$, and define the transpose, the trace, the tensor inner product, and the deviatoric tensor, respectively, as

$$\boldsymbol{\tau}^t := (\tau_{ji})_{i,j=1,n}, \quad \operatorname{tr}(\boldsymbol{\tau}) := \sum_{i=1}^n \tau_{ii}, \quad \boldsymbol{\tau} : \boldsymbol{\zeta} := \sum_{i,j=1}^n \tau_{ij} \zeta_{ij}, \quad \text{and} \quad \boldsymbol{\tau}^d := \boldsymbol{\tau} - \frac{1}{n} \operatorname{tr}(\boldsymbol{\tau}) \mathbb{I},$$

where \mathbb{I} is the identity tensor in $\mathbb{R} := \mathbb{R}^{n \times n}$. In what follows, when no confusion arises, $|\cdot|$ will denote the Euclidean norm in $\mathbf{R} := \mathbb{R}^n$ or $\mathbb{R} := \mathbb{R}^{n \times n}$. Additionally, given $p > 1$, we define the following vectorial and tensorial functional spaces (see [5, Section 2.2] for details):

$$\mathbf{H}(\operatorname{div}_p; \Omega) := \left\{ \boldsymbol{\eta} \in \mathbf{L}^2(\Omega) : \operatorname{div}(\boldsymbol{\eta}) \in L^p(\Omega) \right\}$$

and

$$\mathbb{H}(\mathbf{div}_p; \Omega) := \left\{ \boldsymbol{\tau} \in \mathbb{L}^2(\Omega) : \mathbf{div}(\boldsymbol{\tau}) \in L^p(\Omega) \right\},$$

endowed with the norms

$$\|\boldsymbol{\eta}\|_{\operatorname{div}_p; \Omega} := \|\boldsymbol{\eta}\|_{0,\Omega} + \|\operatorname{div}(\boldsymbol{\eta})\|_{0,p;\Omega} \quad \text{and} \quad \|\boldsymbol{\tau}\|_{\mathbf{div}_p; \Omega} := \|\boldsymbol{\tau}\|_{0,\Omega} + \|\mathbf{div}(\boldsymbol{\tau})\|_{0,p;\Omega},$$

respectively. In addition, $H^{1/2}(\Gamma)$ is the space of traces of functions of $H^1(\Omega)$ and $H^{-1/2}(\Gamma)$ denotes its dual. Also, by $\langle \cdot, \cdot \rangle_\Gamma$ we will denote the corresponding product of duality between $H^{-1/2}(\Gamma)$ and $H^{1/2}(\Gamma)$ (and also between $\mathbf{H}^{-1/2}(\Gamma)$ and $\mathbf{H}^{1/2}(\Gamma)$).

2 The model problem and its variational formulation

In this section we recall from [5] the model problem, its corresponding fully-mixed variational formulation, and the associated mixed finite element method.

2.1 The coupling of the Brinkman–Forchheimer and double-diffusion equations

In what follows we consider the model introduced in [29] (see also [8, 5]), which is given by a steady double-diffusive convection system in a fluid saturated porous medium. More precisely, we focus on solving the coupling of the incompressible Brinkman–Forchheimer and double-diffusion equations, which reduces to finding a velocity field \mathbf{u} , a pressure field p , a temperature field ϕ_1 and a concentration field ϕ_2 , both defining a vector $\phi := (\phi_1, \phi_2)$, such that

$$\begin{aligned} -\nu \Delta \mathbf{u} + \mathbf{K}^{-1} \mathbf{u} + \mathbf{F} |\mathbf{u}| \mathbf{u} + \nabla p &= \mathbf{f}(\phi) \quad \text{in } \Omega, \quad \operatorname{div}(\mathbf{u}) = 0 \quad \text{in } \Omega, \\ -\operatorname{div}(\mathbf{Q}_1 \nabla \phi_1) + \mathbf{R}_1 \mathbf{u} \cdot \nabla \phi_1 &= 0 \quad \text{in } \Omega, \quad -\operatorname{div}(\mathbf{Q}_2 \nabla \phi_2) + \mathbf{R}_2 \mathbf{u} \cdot \nabla \phi_2 = 0 \quad \text{in } \Omega, \\ \mathbf{u} &= \mathbf{u}_D, \quad \phi_1 = \phi_{1,D}, \quad \text{and} \quad \phi_2 = \phi_{2,D} \quad \text{on } \Gamma, \quad \int_\Omega p = 0, \end{aligned} \quad (2.1)$$

with parameters $\nu := D_a \tilde{\mu} / \mu$ and $\mathbf{F} := \vartheta D_a \mathbf{R}_1$, where D_a stands for the Darcy number, $\tilde{\mu}$ the viscosity, μ the effective viscosity, \mathbf{R}_1 the thermal Rayleigh number, \mathbf{R}_2 the solute Rayleigh number, and ϑ is a real number that can be calculated experimentally. In addition, the Dirichlet boundary data is given by $\mathbf{u}_D \in \mathbf{H}^{1/2}(\Gamma)$, $\phi_{1,D} \in H^{1/2}(\Gamma)$ and $\phi_{2,D} \in H^{1/2}(\Gamma)$. Owing to the incompressibility of the fluid and the Dirichlet boundary condition for \mathbf{u} , the datum \mathbf{u}_D must satisfy the compatibility condition

$$\int_\Gamma \mathbf{u}_D \cdot \mathbf{n} = 0. \quad (2.2)$$

In turn, the external force \mathbf{f} is defined by

$$\mathbf{f}(\phi) := -(\phi_1 - \phi_{1,r}) \mathbf{g} + \frac{1}{\varrho} (\phi_2 - \phi_{2,r}) \mathbf{g}, \quad (2.3)$$

with \mathbf{g} representing the potential type gravitational acceleration, $\phi_{1,r}$ the reference temperature, $\phi_{2,r}$ the reference concentration of a solute, both of them living in $L^6(\Omega)$, and ϱ is another parameter experimentally valued that can be assumed to be greater than 1 (see [29, Section 2] for details). In turn, the permeability, and the thermal diffusion and concentration diffusion tensors, are denoted by \mathbf{K} , \mathbf{Q}_1 and \mathbf{Q}_2 , respectively, all them lying in $\mathbb{L}^\infty(\Omega)$. Moreover, the inverse of \mathbf{K} and tensors \mathbf{Q}_1 , \mathbf{Q}_2 , are uniformly positive definite tensors, which means that there exist positive constants $C_{\mathbf{K}}$, $C_{\mathbf{Q}_1}$, and $C_{\mathbf{Q}_2}$, such that

$$\mathbf{v} \cdot \mathbf{K}^{-1}(\mathbf{x}) \mathbf{v} \geq C_{\mathbf{K}} |\mathbf{v}|^2 \quad \text{and} \quad \mathbf{v} \cdot \mathbf{Q}_j(\mathbf{x}) \mathbf{v} \geq C_{\mathbf{Q}_j} |\mathbf{v}|^2 \quad \forall \mathbf{v} \in \mathbb{R}^n, \quad \forall \mathbf{x} \in \Omega, \quad j \in \{1, 2\}. \quad (2.4)$$

Next, we introduce the velocity gradient \mathbf{t} , the pseudostress tensor $\boldsymbol{\sigma}$, the temperature/concentration gradient $\tilde{\mathbf{t}}_j$, and suitable auxiliary variables $\boldsymbol{\rho}_j$ depending on $\tilde{\mathbf{t}}_j$, \mathbf{u} , and ϕ_j , all of which are defined, respectively, by

$$\mathbf{t} := \nabla \mathbf{u}, \quad \boldsymbol{\sigma} := \nu \mathbf{t} - p \mathbb{I}, \quad \tilde{\mathbf{t}}_j := \nabla \phi_j, \quad \boldsymbol{\rho}_j := \mathbf{Q}_j \tilde{\mathbf{t}}_j - \frac{1}{2} \mathbf{R}_j \phi_j \mathbf{u}, \quad \forall j \in \{1, 2\}, \quad \text{in } \Omega. \quad (2.5)$$

In this way, utilizing the incompressibility condition (cf. second eq. in (2.1)) to eliminate the pressure, which can be computed afterwards as

$$p = -\frac{1}{n} \operatorname{tr}(\boldsymbol{\sigma}) \quad \text{in } \Omega, \quad (2.6)$$

we find that problem (2.1) can be rewritten, equivalently, as follows: Find $(\mathbf{u}, \mathbf{t}, \boldsymbol{\sigma})$ and $(\phi_j, \tilde{\mathbf{t}}_j, \boldsymbol{\rho}_j), j \in \{1, 2\}$, in suitable spaces to be indicated below such that

$$\begin{aligned} \mathbf{t} &= \nabla \mathbf{u} \quad \text{in } \Omega, \quad \boldsymbol{\sigma}^d = \nu \mathbf{t} \quad \text{in } \Omega, \quad \mathbf{K}^{-1} \mathbf{u} + \mathbb{F} |\mathbf{u}| \mathbf{u} - \operatorname{div}(\boldsymbol{\sigma}) = \mathbf{f}(\phi) \quad \text{in } \Omega, \\ \tilde{\mathbf{t}}_j &= \nabla \phi_j \quad \text{in } \Omega, \quad \mathbf{Q}_j \tilde{\mathbf{t}}_j - \frac{1}{2} \mathbf{R}_j \phi_j \mathbf{u} = \boldsymbol{\rho}_j \quad \text{in } \Omega, \quad \frac{1}{2} \mathbf{R}_j \mathbf{u} \cdot \tilde{\mathbf{t}}_j - \operatorname{div}(\boldsymbol{\rho}_j) = 0 \quad \text{in } \Omega, \\ \mathbf{u} &= \mathbf{u}_D \quad \text{and} \quad \phi = \phi_D \quad \text{on } \Gamma, \quad \int_{\Omega} \operatorname{tr}(\boldsymbol{\sigma}) = 0. \end{aligned} \quad (2.7)$$

where the Dirichlet datum for ϕ is certainly given by $\phi_D := (\phi_{1,D}, \phi_{2,D})$. Note that (2.6) and the last equation of (2.7) establish that $\int_{\Omega} p = 0$, which is required for purposes of uniqueness of this unknown.

2.2 The fully-mixed variational formulation

We first recall from [5, Section 2.2] the following tensorial functional spaces

$$\begin{aligned} \mathbb{L}_{\operatorname{tr}}^2(\Omega) &:= \left\{ \mathbf{r} \in \mathbb{L}^2(\Omega) : \operatorname{tr}(\mathbf{r}) = 0 \quad \text{in } \Omega \right\}, \\ \mathbb{H}_0(\operatorname{div}_{3/2}; \Omega) &:= \left\{ \boldsymbol{\tau} \in \mathbb{H}(\operatorname{div}_{3/2}; \Omega) : \int_{\Omega} \operatorname{tr}(\boldsymbol{\tau}) = 0 \right\}, \end{aligned}$$

and observe that the following decomposition holds:

$$\mathbb{H}(\operatorname{div}_{3/2}; \Omega) = \mathbb{H}_0(\operatorname{div}_{3/2}; \Omega) \oplus \mathbb{R}\mathbb{I}. \quad (2.8)$$

Next, for the sake of clarity, we set the notations

$$\begin{aligned} \vec{\mathbf{u}} &:= (\mathbf{u}, \mathbf{t}), \quad \vec{\mathbf{v}} := (\mathbf{v}, \mathbf{r}), \quad \vec{\mathbf{w}} := (\mathbf{w}, \mathbf{s}) \in \mathbf{H} := \mathbf{L}^3(\Omega) \times \mathbb{L}_{\operatorname{tr}}^2(\Omega), \\ \vec{\phi}_j &:= (\phi_j, \tilde{\mathbf{t}}_j), \quad \vec{\psi}_j := (\psi_j, \tilde{\mathbf{r}}_j) \in \tilde{\mathbf{H}} := \mathbf{L}^6(\Omega) \times \mathbf{L}^2(\Omega). \end{aligned}$$

where the product spaces \mathbf{H} and $\tilde{\mathbf{H}}$ are endowed, respectively, with the norms

$$\|\vec{\mathbf{v}}\| := \|\mathbf{v}\|_{0,3;\Omega} + \|\mathbf{r}\|_{0,\Omega} \quad \forall \vec{\mathbf{v}} \in \mathbf{H} \quad \text{and} \quad \|\vec{\psi}_j\| := \|\psi_j\|_{0,6;\Omega} + \|\tilde{\mathbf{r}}_j\|_{0,\Omega} \quad \forall \vec{\psi}_j \in \tilde{\mathbf{H}}.$$

Hence, proceeding as in [5, eq. (2.27)], that is, multiplying the first two rows of equations in (2.7) by suitable test functions, integrating by parts, using (2.2) and the Dirichlet boundary conditions, we find that the fully-mixed variational formulation of (2.7) reduces to: Find $(\vec{\mathbf{u}}, \boldsymbol{\sigma}) \in \mathbf{H} \times \mathbb{H}_0(\operatorname{div}_{3/2}; \Omega)$ and $(\vec{\phi}_j, \boldsymbol{\rho}_j) \in \tilde{\mathbf{H}} \times \mathbf{H}(\operatorname{div}_{6/5}; \Omega), j \in \{1, 2\}$, such that

$$\begin{aligned} [a(\vec{\mathbf{u}}), \vec{\mathbf{v}}] + [b(\vec{\mathbf{v}}), \boldsymbol{\sigma}] &= [F_{\phi}, \vec{\mathbf{v}}] \quad \forall \vec{\mathbf{v}} \in \mathbf{H}, \\ [b(\vec{\mathbf{u}}), \boldsymbol{\tau}] &= [G_D, \boldsymbol{\tau}] \quad \forall \boldsymbol{\tau} \in \mathbb{H}_0(\operatorname{div}_{3/2}; \Omega), \\ [\tilde{a}_j(\vec{\phi}_j), \vec{\psi}_j] + [c_j(\mathbf{u})(\vec{\phi}_j), \vec{\psi}_j] + [\tilde{b}(\vec{\psi}_j), \boldsymbol{\rho}_j] &= 0 \quad \forall \vec{\psi}_j \in \tilde{\mathbf{H}}, \\ [\tilde{b}(\vec{\phi}_j), \boldsymbol{\eta}_j] &= [\tilde{G}_j, \boldsymbol{\eta}_j] \quad \forall \boldsymbol{\eta}_j \in \mathbf{H}(\operatorname{div}_{6/5}; \Omega), \end{aligned} \quad (2.9)$$

where the operators a , b , \tilde{a}_j , \tilde{b} , and $c_j(\mathbf{w})$, for a given $\mathbf{w} \in \mathbf{L}^3(\Omega)$, are defined, respectively, as

$$[a(\vec{\mathbf{w}}), \vec{\mathbf{v}}] := \int_{\Omega} \mathbf{K}^{-1} \mathbf{w} \cdot \mathbf{v} + \mathbb{F} \int_{\Omega} |\mathbf{w}| \mathbf{w} \cdot \mathbf{v} + \nu \int_{\Omega} \mathbf{s} : \mathbf{r}, \quad (2.10)$$

$$[b(\vec{\mathbf{v}}), \boldsymbol{\tau}] := - \int_{\Omega} \mathbf{v} \cdot \operatorname{div}(\boldsymbol{\tau}) - \int_{\Omega} \boldsymbol{\tau} : \mathbf{r}, \quad (2.11)$$

$$[\tilde{a}_j(\vec{\phi}_j), \vec{\psi}_j] := \int_{\Omega} \mathbf{Q}_j \tilde{\mathbf{t}}_j \cdot \tilde{\mathbf{r}}_j, \quad [\tilde{b}(\vec{\psi}_j), \boldsymbol{\eta}_j] := - \int_{\Omega} \psi_j \operatorname{div}(\boldsymbol{\eta}_j) - \int_{\Omega} \boldsymbol{\eta}_j \cdot \tilde{\mathbf{r}}_j, \quad (2.12)$$

and

$$[c_j(\mathbf{w})(\vec{\phi}_j), \vec{\psi}_j] := \frac{1}{2} \mathbb{R}_j \left\{ \int_{\Omega} \psi_j \mathbf{w} \cdot \tilde{\mathbf{t}}_j - \int_{\Omega} \phi_j \mathbf{w} \cdot \tilde{\mathbf{r}}_j \right\}, \quad (2.13)$$

for all $\vec{\mathbf{w}} = (\mathbf{w}, \mathbf{s})$, $\vec{\mathbf{v}} = (\mathbf{v}, \mathbf{r}) \in \mathbf{H}$, $\boldsymbol{\tau} \in \mathbb{H}_0(\operatorname{div}_{3/2}; \Omega)$ and for all $\vec{\phi}_j := (\phi_j, \tilde{\mathbf{t}}_j)$, $\vec{\psi}_j := (\psi_j, \tilde{\mathbf{r}}_j) \in \tilde{\mathbf{H}}$, $\boldsymbol{\eta}_j \in \mathbf{H}(\operatorname{div}_{6/5}; \Omega)$. In turn, given $\boldsymbol{\varphi} = (\varphi_1, \varphi_2) \in \mathbf{L}^6(\Omega)$, $F_{\boldsymbol{\varphi}}$, $G_{\mathbb{D}}$, and \tilde{G}_j are the bounded linear functionals defined by

$$[F_{\boldsymbol{\varphi}}, \vec{\mathbf{v}}] := \int_{\Omega} \mathbf{f}(\boldsymbol{\varphi}) \cdot \mathbf{v}, \quad [G_{\mathbb{D}}, \boldsymbol{\tau}] := - \langle \boldsymbol{\tau} \mathbf{n}, \mathbf{u}_{\mathbb{D}} \rangle_{\Gamma}, \quad (2.14)$$

and

$$[\tilde{G}_j, \boldsymbol{\eta}_j] := - \langle \boldsymbol{\eta}_j \cdot \mathbf{n}, \phi_{j,\mathbb{D}} \rangle_{\Gamma}, \quad (2.15)$$

for all $\vec{\mathbf{v}} = (\mathbf{v}, \mathbf{r}) \in \mathbf{H}$, $\boldsymbol{\tau} \in \mathbb{H}_0(\operatorname{div}_{3/2}; \Omega)$ and for all $\boldsymbol{\eta}_j \in \mathbf{H}(\operatorname{div}_{6/5}; \Omega)$. In all the terms above, $[\cdot, \cdot]$ denotes the duality pairing induced by the corresponding operators.

The well-posedness of (2.9), which makes use of a fixed-point strategy along with classical results on nonlinear monotone operators and the Babuška–Brezzi theory in Banach spaces, is established by [5, Theorem 3.13]. More precisely, given $r > 0$, and under smallness assumptions on the data involving r , namely those detailed in [5, eqs. (3.41) and (3.49)], it is proved that a suitable operator mapping the ball $\mathbf{W} := \left\{ \mathbf{w} \in \mathbf{L}^3(\Omega) : \|\mathbf{w}\|_{0,3;\Omega} \leq r \right\}$ into itself, has a unique fixed-point \mathbf{u} in it, which yields the unique solution

$$(\vec{\mathbf{u}}, \boldsymbol{\sigma}, \vec{\phi}_j, \boldsymbol{\rho}_j) \in \mathbf{H} \times \mathbb{H}_0(\operatorname{div}_{3/2}; \Omega) \times \tilde{\mathbf{H}} \times \mathbf{H}(\operatorname{div}_{6/5}; \Omega), \quad j \in \{1, 2\},$$

of (2.9). In particular, note that there certainly holds

$$\|\mathbf{u}\|_{0,3;\Omega} \leq r. \quad (2.16)$$

2.3 The finite element method

We let $\{\mathcal{T}_h\}_{h>0}$ be a regular family of triangulations of $\bar{\Omega}$, which are made of triangles T (when $n = 2$) or tetrahedra (when $n = 3$) of diameter h_T , and define the meshsize $h := \max \{h_T : T \in \mathcal{T}_h\}$. In turn, given an integer $l \geq 0$ and a subset S of \mathbb{R}^n , we denote by $\mathbf{P}_l(S)$ the space of polynomials of degree $\leq l$ defined on S , with vector and tensor versions denoted by $\mathbf{P}_l(S) := [\mathbf{P}_l(S)]^n$ and $\mathbb{P}_l(S) := [\mathbf{P}_l(S)]^{n \times n}$, respectively. Hence, for each integer $k \geq 0$ and for each $T \in \mathcal{T}_h$, we define the local Raviart–Thomas space of order k as

$$\mathbf{RT}_k(T) := \mathbf{P}_k(T) \oplus \tilde{\mathbf{P}}_k(T) \mathbf{x},$$

where $\mathbf{x} := (x_1, \dots, x_n)^{\dagger}$ is a generic vector of \mathbb{R}^n , $\tilde{\mathbf{P}}_k(T)$ is the space of polynomials of total degree equal to k defined on T . Next, recalling from [5, Section 4.1] the finite element spaces

$$\begin{aligned}
\mathbf{H}_h^{\mathbf{u}} &:= \left\{ \mathbf{v}_h \in \mathbf{L}^3(\Omega) : \mathbf{v}_h|_T \in \mathbf{P}_k(T) \quad \forall T \in \mathcal{T}_h \right\}, \\
\mathbb{H}_h^{\mathbf{t}} &:= \left\{ \mathbf{r}_h \in \mathbb{L}_{\text{tr}}^2(\Omega) : \mathbf{r}_h|_T \in \mathbb{P}_k(T) \quad \forall T \in \mathcal{T}_h \right\}, \\
\mathbb{H}_h^{\sigma} &:= \left\{ \boldsymbol{\tau}_h \in \mathbb{H}_0(\mathbf{div}_{3/2}; \Omega) : \mathbf{c}^{\text{t}} \boldsymbol{\tau}_h|_T \in \mathbf{RT}_k(T) \quad \forall \mathbf{c} \in \mathbb{R}^n, \quad \forall T \in \mathcal{T}_h \right\}, \\
\mathbf{H}_h^{\phi} &:= \left\{ \psi_h \in \mathbf{L}^6(\Omega) : \psi_h|_T \in \mathbf{P}_k(T) \quad \forall T \in \mathcal{T}_h \right\}, \\
\mathbf{H}_h^{\tilde{\mathbf{t}}} &:= \left\{ \tilde{\mathbf{r}}_h \in \mathbf{L}^2(\Omega) : \tilde{\mathbf{r}}_h|_T \in \mathbf{P}_k(T) \quad \forall T \in \mathcal{T}_h \right\}, \\
\mathbf{H}_h^{\rho} &:= \left\{ \boldsymbol{\eta}_h \in \mathbf{H}(\mathbf{div}_{6/5}; \Omega) : \boldsymbol{\eta}_h|_T \in \mathbf{RT}_k(T) \quad \forall T \in \mathcal{T}_h \right\},
\end{aligned} \tag{2.17}$$

and denoting from now on

$$\begin{aligned}
\boldsymbol{\phi}_h &:= (\phi_{1,h}, \phi_{2,h}), \quad \boldsymbol{\varphi}_h := (\varphi_{1,h}, \varphi_{2,h}) \in \mathbf{H}_h^{\phi} := \mathbf{H}_h^{\phi} \times \mathbf{H}_h^{\phi}, \\
\tilde{\mathbf{u}}_h &:= (\mathbf{u}_h, \mathbf{t}_h), \quad \tilde{\mathbf{v}}_h := (\mathbf{v}_h, \mathbf{r}_h) \in \mathbf{H}_h := \mathbf{H}_h^{\mathbf{u}} \times \mathbb{H}_h^{\mathbf{t}}, \\
\tilde{\boldsymbol{\phi}}_{j,h} &:= (\phi_{j,h}, \tilde{\mathbf{t}}_{j,h}), \quad \tilde{\boldsymbol{\psi}}_{j,h} := (\psi_{j,h}, \tilde{\mathbf{r}}_{j,h}) \in \tilde{\mathbf{H}}_h := \mathbf{H}_h^{\phi} \times \mathbf{H}_h^{\tilde{\mathbf{t}}},
\end{aligned}$$

the Galerkin scheme for (2.9) reads: Find $(\tilde{\mathbf{u}}_h, \boldsymbol{\sigma}_h) \in \mathbf{H}_h \times \mathbb{H}_h^{\sigma}$ and $(\tilde{\boldsymbol{\phi}}_{j,h}, \boldsymbol{\rho}_{j,h}) \in \tilde{\mathbf{H}}_h \times \mathbf{H}_h^{\rho}$, $j \in \{1, 2\}$, such that

$$\begin{aligned}
[a(\tilde{\mathbf{u}}_h), \tilde{\mathbf{v}}_h] + [b(\tilde{\mathbf{v}}_h), \boldsymbol{\sigma}_h] &= [F_{\boldsymbol{\phi}_h}, \tilde{\mathbf{v}}_h] \quad \forall \tilde{\mathbf{v}}_h \in \mathbf{H}_h, \\
[b(\tilde{\mathbf{u}}_h), \boldsymbol{\tau}_h] &= [G_{\text{D}}, \boldsymbol{\tau}_h] \quad \forall \boldsymbol{\tau}_h \in \mathbb{H}_h^{\sigma}, \\
[\tilde{a}_j(\tilde{\boldsymbol{\phi}}_{j,h}), \tilde{\boldsymbol{\psi}}_{j,h}] + [c_j(\mathbf{u}_h)(\tilde{\boldsymbol{\phi}}_{j,h}), \tilde{\boldsymbol{\psi}}_{j,h}] + [\tilde{b}(\tilde{\boldsymbol{\psi}}_{j,h}), \boldsymbol{\rho}_{j,h}] &= 0 \quad \forall \tilde{\boldsymbol{\psi}}_{j,h} \in \tilde{\mathbf{H}}_h, \\
[\tilde{b}(\tilde{\boldsymbol{\phi}}_{j,h}), \boldsymbol{\eta}_{j,h}] &= [\tilde{G}_j, \boldsymbol{\eta}_{j,h}] \quad \forall \boldsymbol{\eta}_{j,h} \in \mathbf{H}_h^{\rho}.
\end{aligned} \tag{2.18}$$

The solvability analysis and *a priori* error bounds for (2.18) are established in [5, Theorems 4.10 and 5.5], respectively. Indeed, similarly as remarked at the end of Section 2.2, and under the discrete analogues of the assumptions [5, eqs. (3.41) and (3.49)], which are detailed in [5, eqs. (4.23) and (4.26)], it is proved that a suitable discrete operator mapping the ball $\mathbf{W}_h := \left\{ \mathbf{w}_h \in \mathbf{H}_h^{\mathbf{u}} : \|\mathbf{w}_h\|_{0,3;\Omega} \leq r \right\}$ into itself, has a unique fixed-point \mathbf{u}_h in it, which yields the unique solution

$$(\tilde{\mathbf{u}}_h, \boldsymbol{\sigma}_h, \tilde{\boldsymbol{\phi}}_{j,h}, \boldsymbol{\rho}_{j,h}) \in \mathbf{H}_h \times \mathbb{H}_h^{\sigma} \times \tilde{\mathbf{H}}_h \times \mathbf{H}_h^{\rho}, \quad j \in \{1, 2\},$$

of (2.18). Certainly, in this case there also holds

$$\|\mathbf{u}_h\|_{0,3;\Omega} \leq r. \tag{2.19}$$

3 A posteriori error analysis: The 2D case

In this section we derive a reliable and efficient residual-based *a posteriori* error estimator for the two-dimensional version of the Galerkin scheme (2.18). The corresponding *a posteriori* error analysis for the 3D case, which follows from minor modifications of the one to be presented next, will be addressed in Section 4.

3.1 Preliminaries for reliability

We start by introducing a few useful notations for describing local information on elements and edges. First, given $T \in \mathcal{T}_h$, we let $\mathcal{E}(T)$ be the set of edges of T , and denote by \mathcal{E}_h the set of all edges of \mathcal{T}_h , with corresponding diameters denoted by h_e . Then, we set $\mathcal{E}_h = \mathcal{E}_h(\Omega) \cup \mathcal{E}_h(\Gamma)$, where $\mathcal{E}_h(\Omega) := \{e \in \mathcal{E}_h : e \subseteq \Omega\}$ and $\mathcal{E}_h(\Gamma) := \{e \in \mathcal{E}_h : e \subseteq \Gamma\}$. Also for each $e \in \mathcal{E}_h$ we fix unit normal and tangential vectors to e denoted by $\mathbf{n}_e := (n_1, n_2)^t$ and $\mathbf{s}_e := (-n_2, n_1)^t$, respectively. However, when no confusion arises, we will simply write \mathbf{n} and \mathbf{s} instead of \mathbf{n}_e and \mathbf{s}_e , respectively. In addition, the usual jump operator $[[\cdot]]$ across an internal edge $e \in \mathcal{E}_h(\Omega)$ is defined for piecewise continuous tensor, vector, or scalar-valued functions ζ as simply $[[\zeta]] := \zeta|_T - \zeta|_{T'}$, where T and T' are the triangles of \mathcal{T}_h having e as a common edge. Furthermore, given scalar, vector and matrix valued fields ϕ , $\mathbf{v} := (v_1, v_2)^t$ and $\boldsymbol{\tau} := (\tau_{ij})_{2 \times 2}$, respectively, we let

$$\begin{aligned} \mathbf{curl}(\phi) &:= \left(\frac{\partial \phi}{\partial x_2}, -\frac{\partial \phi}{\partial x_1} \right)^t, & \underline{\mathbf{curl}}(\mathbf{v}) &:= \begin{pmatrix} \mathbf{curl}(v_1)^t \\ \mathbf{curl}(v_2)^t \end{pmatrix}, \\ \mathbf{rot}(\mathbf{v}) &:= \frac{\partial v_2}{\partial x_1} - \frac{\partial v_1}{\partial x_2}, & \mathbf{rot}(\boldsymbol{\tau}) &:= \begin{pmatrix} \mathbf{rot}(\tau_{11}, \tau_{12}) \\ \mathbf{rot}(\tau_{21}, \tau_{22}) \end{pmatrix}, \end{aligned}$$

where the derivatives involved are taken in the distributional sense.

Let us now recall the main properties of the Raviart–Thomas and Clément interpolation operators (cf. [17], [11]). We begin by defining for each $p \geq \frac{2n}{n+2}$ the spaces

$$\mathbf{H}_p := \left\{ \boldsymbol{\tau} \in \mathbf{H}(\operatorname{div}_p; \Omega) : \boldsymbol{\tau}|_T \in \mathbf{W}^{1,p}(T) \quad \forall T \in \mathcal{T}_h \right\}, \quad (3.1)$$

and

$$\widehat{\mathbf{H}}_h^\sigma := \left\{ \boldsymbol{\tau} \in \mathbf{H}(\operatorname{div}_p; \Omega) : \boldsymbol{\tau}|_T \in \mathbf{RT}_k(T) \quad \forall T \in \mathcal{T}_h \right\}. \quad (3.2)$$

In addition, we let $\Pi_h^k : \mathbf{H}_p \rightarrow \widehat{\mathbf{H}}_h^\sigma$ be the Raviart–Thomas interpolation operator, which is characterized for each $\boldsymbol{\tau} \in \mathbf{H}_p$ by the identities (see, e.g. [17, Section 1.2.7])

$$\int_e (\Pi_h^k(\boldsymbol{\tau}) \cdot \mathbf{n}) \xi = \int_e (\boldsymbol{\tau} \cdot \mathbf{n}) \xi \quad \forall \xi \in \mathbf{P}_k(e), \quad \forall \text{edge or face } e \text{ of } \mathcal{T}_h, \quad (3.3)$$

when $k \geq 0$, and

$$\int_T \Pi_h^k(\boldsymbol{\tau}) \cdot \boldsymbol{\psi} = \int_T \boldsymbol{\tau} \cdot \boldsymbol{\psi} \quad \forall \boldsymbol{\psi} \in \mathbf{P}_{k-1}(T), \quad \forall T \in \mathcal{T}_h, \quad (3.4)$$

when $k \geq 1$. In turn, given $q > 1$ such that $\frac{1}{p} + \frac{1}{q} = 1$, we let

$$\mathbf{H}_h^q := \left\{ v \in L^q(\Omega) : v|_T \in \mathbf{P}_k(T) \quad \forall T \in \mathcal{T}_h \right\}, \quad (3.5)$$

and recall from [17, Lemma 1.41] that there holds

$$\operatorname{div}(\Pi_h^k(\boldsymbol{\tau})) = \mathcal{P}_h^k(\operatorname{div}(\boldsymbol{\tau})) \quad \forall \boldsymbol{\tau} \in \mathbf{H}_p, \quad (3.6)$$

where $\mathcal{P}_h^k : L^p(\Omega) \rightarrow \mathbf{H}_h^q$ is the usual orthogonal projector with respect to the $L^2(\Omega)$ -inner product, which satisfies the following error estimate (see [17, Proposition 1.135]): there exists a positive constant C_0 , independent of h , such that for $0 \leq l \leq k+1$ and $1 \leq p \leq \infty$ there holds

$$\|w - \mathcal{P}_h^k(w)\|_{0,p;\Omega} \leq C_0 h^l \|w\|_{l,p;\Omega} \quad \forall w \in \mathbf{W}^{l,p}(\Omega). \quad (3.7)$$

We stress that $\mathcal{P}_h^k(w)|_T = \mathcal{P}_T^k(w|_T) \forall w \in L^p(\Omega)$, where $\mathcal{P}_T^k : L^p(T) \rightarrow P_k(T)$ is the corresponding local orthogonal projector. In addition, denoting by \mathbf{H}_h^u the vector version of \mathbb{H}_h^u (cf. (3.5)), we let $\mathcal{P}_h^k : L^p(\Omega) \rightarrow \mathbf{H}_h^u$ be the vector version of \mathcal{P}_h^k .

Next, we collect some approximation properties of Π_h^k .

Lemma 3.1 *Given $p > 1$, there exist positive constants C_1, C_2 , independent of h , such that for $0 \leq l \leq k$ and for each $T \in \mathcal{T}_h$ there holds*

$$\|\tau - \Pi_h^k(\tau)\|_{0,p;T} \leq C_1 h_T^{l+1} |\tau|_{l+1,p;T} \quad \forall \tau \in \mathbf{W}^{l+1,p}(T), \quad (3.8)$$

and

$$\|\tau \cdot \mathbf{n} - \Pi_h^k(\tau) \cdot \mathbf{n}\|_{0,p;e} \leq C_2 h_e^{1-1/p} |\tau|_{1,p;T} \quad \forall \tau \in \mathbf{W}^{1,p}(T), \quad \forall e \in \mathcal{E}_h(T). \quad (3.9)$$

Proof. For the estimate (3.8) we refer to [23, Lemma 3.1], whereas the proof of (3.9) can be found in [3, Lemma 4.2]. \square

Furthermore, denoting by \mathbb{H}_p and $\widehat{\mathbb{H}}_h^\sigma$ the tensor versions of \mathbf{H}_p (cf. (3.1)) and $\widehat{\mathbf{H}}_h^\sigma$ (cf. (3.2)), respectively, we let $\mathbf{\Pi}_h^k : \mathbb{H}_p \rightarrow \widehat{\mathbb{H}}_h^\sigma$ be the operator Π_h^k acting row-wise. Then, according to the decomposition (2.8), for each $\tau \in \mathbb{H}_p$ there holds

$$\mathbf{\Pi}_h^k(\tau) = \mathbf{\Pi}_{h,0}^k(\tau) + \ell \mathbb{I}, \quad \text{with} \quad \ell := \frac{1}{n|\Omega|} \int_{\Omega} \text{tr}(\mathbf{\Pi}_h^k(\tau)) \in \mathbb{R}$$

$$\text{and} \quad \mathbf{\Pi}_{h,0}^k(\tau) := \mathbf{\Pi}_h^k(\tau) - \ell \mathbb{I} \in \mathbb{H}_h^\sigma.$$

Other approximation properties of Π_h^k and $\mathbf{\Pi}_h^k$, in particular those involving the div and \mathbf{div} operators, and using (3.6) and (3.7), and their tensorial versions with $\mathbf{\Pi}_h^k$ and \mathcal{P}_h^k , can also be derived. However, since they are not employed in what follows, we omit further details on them.

We now recall from [3, Lemma 4.4] a stable Helmholtz decomposition for the nonstandard Banach space $\mathbf{H}(\text{div}_p; \Omega)$, whose particular cases given by $p = 3/2$ and $p = 6/5$ will be selected in the forthcoming analysis. More precisely, we have the following result.

Lemma 3.2 *Given $p > 1$, there exists a positive constant C_p such that for each $\tau \in \mathbf{H}(\text{div}_p; \Omega)$ there exist $\zeta \in \mathbf{W}^{1,p}(\Omega)$ and $\xi \in \mathbf{H}^1(\Omega)$ satisfying*

$$\tau = \zeta + \mathbf{curl}(\xi) \quad \text{in} \quad \Omega \quad \text{and} \quad \|\zeta\|_{1,p;\Omega} + \|\xi\|_{1,\Omega} \leq C_p \|\tau\|_{\text{div}_p;\Omega}.$$

We stress here that the foregoing result is certainly valid for the tensor version $\mathbb{H}(\mathbf{div}_p; \Omega)$ of $\mathbf{H}(\text{div}_p; \Omega)$ as well, and hence in particular for $\mathbb{H}_0(\mathbf{div}_p; \Omega)$. In other words, for each $\tau \in \mathbb{H}_0(\mathbf{div}_p; \Omega)$ there exist $\zeta \in \mathbb{W}^{1,p}(\Omega)$ and $\xi \in \mathbf{H}^1(\Omega)$ such that

$$\tau = \zeta + \mathbf{curl}(\xi) \quad \text{in} \quad \Omega \quad \text{and} \quad \|\zeta\|_{1,p;\Omega} + \|\xi\|_{1,\Omega} \leq C_p \|\tau\|_{\text{div}_p;\Omega}. \quad (3.10)$$

On the other hand, defining $X_h := \{v_h \in C(\overline{\Omega}) : v_h|_T \in P_1(T) \quad \forall T \in \mathcal{T}_h\}$ and denoting by \mathbf{X}_h its vector version, we let $I_h : \mathbf{H}^1(\Omega) \rightarrow X_h$ and $\mathbf{I}_h : \mathbf{H}^1(\Omega) \rightarrow \mathbf{X}_h$ be the usual Clément interpolation operator and its vector version, respectively. Some local properties of I_h , and hence of \mathbf{I}_h , are established in the following lemma (cf. [11]):

Lemma 3.3 *There exist positive constants C_1 and C_2 , such that*

$$\|v - I_h(v)\|_{0,T} \leq C_1 h_T \|v\|_{1,\Delta(T)} \quad \forall T \in \mathcal{T}_h,$$

and

$$\|v - I_h(v)\|_{0,e} \leq C_2 h_e^{1/2} \|v\|_{1,\Delta(e)} \quad \forall e \in \mathcal{E}_h,$$

where $\Delta(T) := \cup\{T' \in \mathcal{T}_h : T' \cap T \neq \emptyset\}$ and $\Delta(e) := \cup\{T' \in \mathcal{T}_h : T' \cap e \neq \emptyset\}$.

3.2 Reliability

Recalling that $(\vec{\mathbf{u}}_h, \boldsymbol{\sigma}_h, \vec{\phi}_{j,h}, \boldsymbol{\rho}_{j,h}) \in \mathbf{H}_h \times \mathbb{H}_h^\sigma \times \tilde{\mathbf{H}}_h \times \mathbf{H}_h^\rho$, $j \in \{1, 2\}$ is the unique solution of the discrete problem (2.18), we define the global *a posteriori* error estimator Θ by

$$\begin{aligned} \Theta = & \left\{ \sum_{T \in \mathcal{T}_h} \Theta_{1,T}^{6/5} \right\}^{5/6} + \left\{ \sum_{T \in \mathcal{T}_h} \Theta_{2,T}^{3/2} \right\}^{2/3} + \left\{ \sum_{T \in \mathcal{T}_h} \Theta_{3,T}^2 \right\}^{1/2} \\ & + \left\{ \sum_{T \in \mathcal{T}_h} \Theta_{4,T}^3 \right\}^{1/3} + \left\{ \sum_{T \in \mathcal{T}_h} \Theta_{5,T}^6 \right\}^{1/6}, \end{aligned} \quad (3.11)$$

where, for each $T \in \mathcal{T}_h$, the local error indicators $\Theta_{1,T}^{6/5}$, $\Theta_{2,T}^{3/2}$, $\Theta_{3,T}^2$, $\Theta_{4,T}^3$, and $\Theta_{5,T}^6$ are defined as:

$$\Theta_{1,T}^{6/5} := \sum_{j=1}^2 \|\operatorname{div}(\boldsymbol{\rho}_{j,h}) - \frac{1}{2} \mathbf{R}_j \mathbf{u}_h \cdot \tilde{\mathbf{t}}_{j,h}\|_{0,6/5;T}^{6/5}, \quad (3.12)$$

$$\Theta_{2,T}^{3/2} := \|\mathbf{f}(\phi_h) + \operatorname{div}(\boldsymbol{\sigma}_h) - \mathbf{K}^{-1} \mathbf{u}_h - \mathbf{F} | \mathbf{u}_h | \mathbf{u}_h\|_{0,3/2;T}^{3/2}, \quad (3.13)$$

$$\begin{aligned} \Theta_{3,T}^2 := & \|\boldsymbol{\sigma}_h^d - \nu \mathbf{t}_h\|_{0,T}^2 + h_T^2 \|\operatorname{rot}(\mathbf{t}_h)\|_{0,T}^2 + \sum_{e \in \mathcal{E}_h(T) \cap \mathcal{E}_h(\Omega)} h_e \|\llbracket \mathbf{t}_h \mathbf{s} \rrbracket\|_{0,e}^2 \\ & + \sum_{e \in \mathcal{E}_h(T) \cap \mathcal{E}_h(\Gamma)} h_e \|\mathbf{t}_h \mathbf{s} - \nabla \mathbf{u}_D \mathbf{s}\|_{0,e}^2 + \sum_{j=1}^2 \left(\|\boldsymbol{\rho}_{j,h} - \mathbf{Q}_j \tilde{\mathbf{t}}_{j,h} + \frac{1}{2} \mathbf{R}_j \phi_{j,h} \mathbf{u}_h\|_{0,T}^2 \right. \end{aligned} \quad (3.14)$$

$$\begin{aligned} & \left. + h_T^2 \|\operatorname{rot}(\tilde{\mathbf{t}}_{j,h})\|_{0,T}^2 + \sum_{e \in \mathcal{E}_h(T) \cap \mathcal{E}_h(\Omega)} h_e \|\llbracket \tilde{\mathbf{t}}_{j,h} \cdot \mathbf{s} \rrbracket\|_{0,e}^2 + \sum_{e \in \mathcal{E}_h(T) \cap \mathcal{E}_h(\Gamma)} h_e \|\tilde{\mathbf{t}}_{j,h} \cdot \mathbf{s} - \nabla \phi_{j,D} \cdot \mathbf{s}\|_{0,e}^2 \right), \\ \Theta_{4,T}^3 := & h_T^3 \|\mathbf{t}_h - \nabla \mathbf{u}_h\|_{0,3;T}^3 + \sum_{e \in \mathcal{E}_h(T) \cap \mathcal{E}_h(\Gamma)} h_e \|\mathbf{u}_D - \mathbf{u}_h\|_{0,3;e}^3, \end{aligned} \quad (3.15)$$

and

$$\Theta_{5,T}^6 := \sum_{j=1}^2 \left(h_T^6 \|\tilde{\mathbf{t}}_{j,h} - \nabla \phi_{j,h}\|_{0,6;T}^6 + \sum_{e \in \mathcal{E}_h(T) \cap \mathcal{E}_h(\Gamma)} h_e \|\phi_{j,D} - \phi_{j,h}\|_{0,6;e}^6 \right). \quad (3.16)$$

Notice that the fourth and eighth terms in (3.14) require $(\nabla \mathbf{u}_D \mathbf{s})|_e \in \mathbf{L}^2(e)$ and $(\nabla \phi_{j,D} \cdot \mathbf{s})|_e \in \mathbf{L}^2(e)$ for all $e \in \mathcal{E}_h(\Gamma)$, respectively, which is overcome below by simply assuming that $\mathbf{u}_D \in \mathbf{H}^1(\Gamma)$ and $\phi_{j,D} \in \mathbf{H}^1(\Gamma)$, $j \in \{1, 2\}$.

Throughout the rest of the paper, given any $r > 0$, as specified at the end of Sections 2.2 and 2.3, both $c(r)$ and $C(r)$, with or without sub-indexes, denote positive constants depending on r , and eventually on other constants or parameters.

The main result of this section, which establishes the reliability of Θ , reads as follows.

Theorem 3.4 *There exists a constant $C(r) > 0$ such that, under the data assumption*

$$C(r) \|\mathbf{g}\|_{0,\Omega} \|\phi_D\|_{1/2,\Gamma} \leq \frac{1}{2}, \quad (3.17)$$

there holds

$$\|(\vec{\mathbf{u}}, \boldsymbol{\sigma}) - (\vec{\mathbf{u}}_h, \boldsymbol{\sigma}_h)\| + \sum_{j=1}^2 \|(\vec{\phi}_j, \boldsymbol{\rho}_j) - (\vec{\phi}_{j,h}, \boldsymbol{\rho}_{j,h})\| \leq C_{\text{rel}} \Theta, \quad (3.18)$$

where C_{rel} is a positive constant, independent of h .

We begin the proof of Theorem (3.4) with a preliminary estimate for the error $\|(\bar{\mathbf{u}}, \boldsymbol{\sigma}) - (\bar{\mathbf{u}}_h, \boldsymbol{\sigma}_h)\|$. Indeed, proceeding analogously to [9, Section 5.1] (see also [16, Section 1]), we first introduce the residual functionals $\mathcal{Q} : \mathbf{H} \rightarrow \mathbb{R}$ and $\mathcal{R} : \mathbb{H}_0(\mathbf{div}_{3/2}; \Omega) \rightarrow \mathbb{R}$, defined by

$$\mathcal{Q}(\vec{\mathbf{v}}) := [F_{\phi_h}, \vec{\mathbf{v}}] - [a(\bar{\mathbf{u}}_h), \vec{\mathbf{v}}] - [b(\vec{\mathbf{v}}), \boldsymbol{\sigma}_h] \quad \forall \vec{\mathbf{v}} \in \mathbf{H}, \quad (3.19)$$

and

$$\mathcal{R}(\boldsymbol{\tau}) := [G_D, \boldsymbol{\tau}] - [b(\bar{\mathbf{u}}_h), \boldsymbol{\tau}] \quad \forall \boldsymbol{\tau} \in \mathbb{H}_0(\mathbf{div}_{3/2}; \Omega), \quad (3.20)$$

respectively, which, according to the first and second equations of the discrete problem (2.18), satisfy

$$\mathcal{Q}(\vec{\mathbf{v}}_h) = 0 \quad \forall \vec{\mathbf{v}}_h \in \mathbf{H}_h \quad \text{and} \quad \mathcal{R}(\boldsymbol{\tau}_h) = 0 \quad \forall \boldsymbol{\tau}_h \in \mathbb{H}_h^\sigma. \quad (3.21)$$

The announced preliminary result is established as follows.

Lemma 3.5 *There exist $C_1(r), C_2(r) > 0$, independent of h , such that*

$$\|(\bar{\mathbf{u}}, \boldsymbol{\sigma}) - (\bar{\mathbf{u}}_h, \boldsymbol{\sigma}_h)\| \leq C_1(r) \left\{ \|\mathcal{Q}\| + \|\mathcal{R}\| + \|\mathcal{R}\|^2 \right\} + C_2(r) \|\mathbf{g}\|_{0,\Omega} \|\phi - \phi_h\|_{0,6;\Omega}. \quad (3.22)$$

Proof. First, from the first two equations of (2.9) and the definition of \mathcal{Q} and \mathcal{R} (cf. (3.19) and (3.20)), it is clear that

$$[a(\bar{\mathbf{u}}) - a(\bar{\mathbf{u}}_h), \vec{\mathbf{v}}] + [b(\vec{\mathbf{v}}), \boldsymbol{\sigma} - \boldsymbol{\sigma}_h] = [F_\phi - F_{\phi_h}, \vec{\mathbf{v}}] + \mathcal{Q}(\vec{\mathbf{v}}) \quad \forall \vec{\mathbf{v}} \in \mathbf{H}, \quad (3.23)$$

and

$$[b(\bar{\mathbf{u}} - \bar{\mathbf{u}}_h), \boldsymbol{\tau}] = \mathcal{R}(\boldsymbol{\tau}) \quad \forall \boldsymbol{\tau} \in \mathbb{H}_0(\mathbf{div}_{3/2}; \Omega). \quad (3.24)$$

Thus, proceeding similarly to [5, eqs. (3.5)-(3.6) in Theorem 3.1], we employ the continuous inf-sup condition for b , which holds with a constant β (cf. [5, eq. (3.15) in Lemma 3.2]), the converse implication of the equivalence provided in [17, Lemma A.42], and (3.24), to deduce that there exists $\vec{\mathbf{w}} := (\mathbf{w}, \mathbf{s}) \in \mathbf{H}$ such that

$$b(\vec{\mathbf{w}}) = b(\bar{\mathbf{u}} - \bar{\mathbf{u}}_h) = \mathcal{R} \quad \text{and} \quad \|\vec{\mathbf{w}}\| \leq \frac{1}{\beta} \|\mathcal{R}\|. \quad (3.25)$$

It follows that the error $\bar{\mathbf{u}} - \bar{\mathbf{u}}_h$ can be decomposed as

$$\bar{\mathbf{u}} - \bar{\mathbf{u}}_h = \bar{\mathbf{z}} + \vec{\mathbf{w}}, \quad (3.26)$$

with $\bar{\mathbf{z}} := \bar{\mathbf{u}} - \bar{\mathbf{u}}_h - \vec{\mathbf{w}} \in \mathbf{V}$. Then, taking $\vec{\mathbf{v}} = \bar{\mathbf{z}}$ in (3.23), we find that

$$[a(\bar{\mathbf{u}}) - a(\bar{\mathbf{u}}_h), \bar{\mathbf{z}}] = [F_\phi - F_{\phi_h}, \bar{\mathbf{z}}] + \mathcal{Q}(\bar{\mathbf{z}}),$$

and hence, subtracting and adding $a(\bar{\mathbf{u}})$, we obtain

$$\begin{aligned} [a(\bar{\mathbf{u}} - \vec{\mathbf{w}}) - a(\bar{\mathbf{u}}_h), \bar{\mathbf{z}}] &= [a(\bar{\mathbf{u}} - \vec{\mathbf{w}}) - a(\bar{\mathbf{u}}), \bar{\mathbf{z}}] + [a(\bar{\mathbf{u}}) - a(\bar{\mathbf{u}}_h), \bar{\mathbf{z}}] \\ &= [a(\bar{\mathbf{u}} - \vec{\mathbf{w}}) - a(\bar{\mathbf{u}}), \bar{\mathbf{z}}] + [F_\phi - F_{\phi_h}, \bar{\mathbf{z}}] + \mathcal{Q}(\bar{\mathbf{z}}). \end{aligned} \quad (3.27)$$

At this point we recall from [5, eq. (3.30)] that a strong monotonicity property of the operator a establishes the existence of a constant α_{BF} such that

$$[a(\bar{\mathbf{x}}) - a(\bar{\mathbf{y}}), \bar{\mathbf{x}} - \bar{\mathbf{y}}] \geq \alpha_{\text{BF}} \|\bar{\mathbf{x}} - \bar{\mathbf{y}}\|^2$$

for all $\vec{\mathbf{x}}, \vec{\mathbf{y}} \in \mathbf{H}$ such that $\vec{\mathbf{x}} - \vec{\mathbf{y}} \in \mathbf{V}$. Then, applying the foregoing inequality to $\vec{\mathbf{x}} = \vec{\mathbf{u}} - \vec{\mathbf{w}}$ and $\vec{\mathbf{y}} = \vec{\mathbf{u}}_h$, and using (3.27), we find that

$$\alpha_{\text{BF}} \|\vec{\mathbf{z}}\|^2 \leq [a(\vec{\mathbf{u}} - \vec{\mathbf{w}}) - a(\vec{\mathbf{u}}, \vec{\mathbf{z}})] + [F_\phi - F_{\phi_h}, \vec{\mathbf{z}}] + \mathcal{Q}(\vec{\mathbf{z}}),$$

from which, making use of the continuity of a , which involves a constant L_{BF} depending on $|\Omega|$, $\|\mathbf{K}^{-1}\|_{0,\infty;\Omega}$, \mathbf{F} , and ν (cf. [5, eq. (3.25)]), and that of F_ϕ (cf. [5, eq. (3.46)]), and then performing simple algebraic computations, we obtain

$$\begin{aligned} \alpha_{\text{BF}} \|\vec{\mathbf{z}}\|^2 &\leq L_{\text{BF}} \left\{ (1 + 2 \|\mathbf{u}\|_{0,3;\Omega}) \|\mathbf{w}\|_{0,3;\Omega} + \|\mathbf{s}\|_{0,\Omega} + \|\mathbf{w}\|_{0,3;\Omega}^2 \right\} \|\vec{\mathbf{z}}\| \\ &\quad + \left\{ \|\mathbf{g}\|_{0,\Omega} \|\phi - \phi_h\|_{0,6;\Omega} + \|\mathcal{Q}\| \right\} \|\vec{\mathbf{z}}\|. \end{aligned}$$

The above estimate, together with the fact that $\|\mathbf{u}\|_{0,3;\Omega}$ is bounded by r (cf. (2.16)), yield

$$\|\vec{\mathbf{z}}\| \leq c_1(r) \left\{ \|\mathcal{Q}\| + \|\vec{\mathbf{w}}\| + \|\vec{\mathbf{w}}\|^2 \right\} + \frac{1}{\alpha_{\text{BF}}} \|\mathbf{g}\|_{0,\Omega} \|\phi - \phi_h\|_{0,6;\Omega}, \quad (3.28)$$

with $c_1(r) > 0$ independent of h , and hence, using (3.26), (3.25) and (3.28), we conclude that

$$\|\vec{\mathbf{u}} - \vec{\mathbf{u}}_h\| \leq \|\vec{\mathbf{z}}\| + \|\vec{\mathbf{w}}\| \leq c_2(r) \left\{ \|\mathcal{Q}\| + \|\mathcal{R}\| + \|\mathcal{R}\|^2 \right\} + \frac{1}{\alpha_{\text{BF}}} \|\mathbf{g}\|_{0,\Omega} \|\phi - \phi_h\|_{0,6;\Omega}, \quad (3.29)$$

with $c_2(r) > 0$ depending only on L_{BF} , α_{BF} , r , and β . On the other hand, applying the continuous inf-sup condition for b (cf. [5, Lemma 3.2, eq. (3.15)]) to $\boldsymbol{\sigma} - \boldsymbol{\sigma}_h$, employing the identity (3.23) to express $[b(\vec{\mathbf{v}}), \boldsymbol{\sigma} - \boldsymbol{\sigma}_h]$, and using again the continuity of a and F_ϕ (cf. [5, eq. (3.25), (3.46)]), we deduce that

$$\begin{aligned} \beta \|\boldsymbol{\sigma} - \boldsymbol{\sigma}_h\|_{\text{div}_{3/2};\Omega} &\leq \sup_{\substack{\vec{\mathbf{v}} \in \mathbf{H} \\ \vec{\mathbf{v}} \neq \mathbf{0}}} \frac{-[a(\vec{\mathbf{u}}) - a(\vec{\mathbf{u}}_h), \vec{\mathbf{v}}] + [F_\phi - F_{\phi_h}, \vec{\mathbf{v}}] + \mathcal{Q}(\vec{\mathbf{v}})}{\|\vec{\mathbf{v}}\|} \\ &\leq L_{\text{BF}} \left\{ 1 + \|\mathbf{u}\|_{0,3;\Omega} + \|\mathbf{u}_h\|_{0,3;\Omega} \right\} \|\vec{\mathbf{u}} - \vec{\mathbf{u}}_h\| + \|\mathbf{g}\|_{0,\Omega} \|\phi - \phi_h\|_{0,6;\Omega} + \|\mathcal{Q}\|, \end{aligned}$$

which, along with the fact that both $\|\mathbf{u}\|_{0,3;\Omega}$ and $\|\mathbf{u}_h\|_{0,3;\Omega}$ are bounded by r (cf. (2.16), (2.19)), and some algebraic manipulations, imply

$$\|\boldsymbol{\sigma} - \boldsymbol{\sigma}_h\|_{\text{div}_{3/2};\Omega} \leq c_3(r) \left\{ \|\vec{\mathbf{u}} - \vec{\mathbf{u}}_h\| + \|\mathcal{Q}\| \right\} + \frac{1}{\beta} \|\mathbf{g}\|_{0,\Omega} \|\phi - \phi_h\|_{0,6;\Omega}, \quad (3.30)$$

with $c_3(r) > 0$ depending only on L_{BF} , r , and β . Therefore, the estimate (3.22) follows from (3.29) and (3.30), thus ending the proof. \square

We continue with a preliminary *a posteriori* estimate for the error $\|(\vec{\phi}_j, \boldsymbol{\rho}_j) - (\vec{\phi}_{j,h}, \boldsymbol{\rho}_{j,h})\|$. To that end, we recall from [5, Section 3.3] that for each $\mathbf{w} \in \mathbf{L}^3(\Omega)$, and $j \in \{1, 2\}$, we define the operator $\tilde{\mathbf{S}}_j(\mathbf{w}) := \phi_j$, where $(\vec{\phi}_j, \boldsymbol{\rho}_j) := ((\phi_j, \tilde{\mathbf{t}}_j), \boldsymbol{\rho}_j)$ is the solution of the problem arising from the last two equations of (2.9) after replacing \mathbf{u} by \mathbf{w} , that is, $(\vec{\phi}_j, \boldsymbol{\rho}_j) \in \tilde{\mathbf{H}} \times \mathbf{H}(\text{div}_{6/5}; \Omega)$ is such that

$$\begin{aligned} [\tilde{a}_j(\vec{\phi}_j), \vec{\psi}_j] + [c_j(\mathbf{w})(\vec{\phi}_j), \vec{\psi}_j] + [\tilde{b}(\vec{\psi}_j), \boldsymbol{\rho}_j] &= 0 \quad \forall \vec{\psi}_j \in \tilde{\mathbf{H}}, \\ [\tilde{b}(\vec{\phi}_j), \boldsymbol{\eta}_j] &= [\tilde{G}_j, \boldsymbol{\eta}_j] \quad \forall \boldsymbol{\eta}_j \in \mathbf{H}(\text{div}_{6/5}; \Omega). \end{aligned} \quad (3.31)$$

In turn, we know from [5, Lemma 3.8] that (3.31) is well-posed for each $\mathbf{w} \in \mathbf{L}^3(\Omega)$, and $j \in \{1, 2\}$, which implies that the bilinear forms arising after adding the corresponding left-hand sides satisfy

global inf-sup conditions uniformly. In other words, denoting from now on $\mathbf{H}_D := \tilde{\mathbf{H}} \times \mathbf{H}(\text{div}_{6/5}; \Omega)$, there exist positive constants γ_j , $j \in \{1, 2\}$, independent of \mathbf{w} , such that

$$\gamma_j \|(\vec{\varphi}_j, \zeta_j)\| \leq \sup_{\substack{(\vec{\psi}_j, \boldsymbol{\eta}_j) \in \mathbf{H}_D \\ (\vec{\psi}_j, \boldsymbol{\eta}_j) \neq \mathbf{0}}} \frac{[\tilde{a}_j(\vec{\varphi}_j), \vec{\psi}_j] + [c_j(\mathbf{w})(\vec{\varphi}_j), \vec{\psi}_j] + [\tilde{b}(\vec{\psi}_j), \zeta_j] + [\tilde{b}(\vec{\varphi}_j), \boldsymbol{\eta}_j]}{\|(\vec{\psi}_j, \boldsymbol{\eta}_j)\|}, \quad (3.32)$$

for all $(\vec{\varphi}_j, \zeta_j) \in \mathbf{H}_D$.

Next, we let $\tilde{\mathcal{Q}}_j : \tilde{\mathbf{H}} \rightarrow \mathbb{R}$ and $\tilde{\mathcal{R}}_j : \mathbf{H}(\text{div}_{6/5}; \Omega) \rightarrow \mathbb{R}$ be the residual functionals defined by

$$\tilde{\mathcal{Q}}_j(\vec{\psi}_j) := -[\tilde{a}(\vec{\phi}_{j,h}), \vec{\psi}_j] - [c_j(\mathbf{u}_h)(\vec{\phi}_{j,h}), \vec{\psi}_j] - [\tilde{b}(\vec{\psi}_j), \boldsymbol{\rho}_{j,h}] \quad \forall \vec{\psi}_j \in \tilde{\mathbf{H}}, \quad (3.33)$$

and

$$\tilde{\mathcal{R}}_j(\boldsymbol{\eta}_j) := [\tilde{G}_j, \boldsymbol{\eta}_j] - [\tilde{b}(\vec{\phi}_{j,h}), \boldsymbol{\eta}_j] \quad \forall \boldsymbol{\eta}_j \in \mathbf{H}(\text{div}_{6/5}; \Omega), \quad (3.34)$$

respectively, and observe, from the third and fourth equations of the discrete problem (2.18), that they satisfy

$$\tilde{\mathcal{Q}}_j(\vec{\psi}_{j,h}) = 0 \quad \forall \vec{\psi}_{j,h} \in \tilde{\mathbf{H}}_h \quad \text{and} \quad \tilde{\mathcal{R}}_j(\boldsymbol{\eta}_{j,h}) = 0 \quad \forall \boldsymbol{\eta}_{j,h} \in \mathbf{H}_h^{\rho}. \quad (3.35)$$

Then, the aforementioned result is established as follows.

Lemma 3.6 *There exists $C_3(r) > 0$, independent of h , such that*

$$\sum_{j=1}^2 \|(\vec{\phi}_j, \boldsymbol{\rho}_j) - (\vec{\phi}_{j,h}, \boldsymbol{\rho}_{j,h})\| \leq C_3(r) \left\{ \sum_{j=1}^2 (\|\tilde{\mathcal{Q}}_j\| + \|\tilde{\mathcal{R}}_j\|) + \|\phi_D\|_{1/2, \Gamma} \|\mathbf{u} - \mathbf{u}_h\|_{0,3;\Omega} \right\}, \quad (3.36)$$

Proof. We proceed similarly to [23, Lemma 3.5]. In fact, applying the inf-sup condition (3.32) to $\mathbf{w} = \mathbf{u}$ and $(\vec{\varphi}_j, \zeta_j) := (\vec{\phi}_j - \vec{\phi}_{j,h}, \boldsymbol{\rho}_j - \boldsymbol{\rho}_{j,h})$, adding and subtracting $[c_j(\mathbf{u}_h)(\vec{\phi}_{j,h}), \vec{\psi}_j]$, using the last two equations of (2.9), and the definitions of $\tilde{\mathcal{Q}}_j$ and $\tilde{\mathcal{R}}_j$ (cf. (3.33), (3.34)), we deduce that

$$\begin{aligned} & \gamma_j \|(\vec{\phi}_j, \boldsymbol{\rho}_j) - (\vec{\phi}_{j,h}, \boldsymbol{\rho}_{j,h})\| \\ & \leq \sup_{\substack{(\vec{\psi}_j, \boldsymbol{\eta}_j) \in \mathbf{H}_D \\ (\vec{\psi}_j, \boldsymbol{\eta}_j) \neq \mathbf{0}}} \frac{\tilde{\mathcal{Q}}_j(\vec{\psi}_j) + \tilde{\mathcal{R}}_j(\boldsymbol{\eta}_j)}{\|(\vec{\psi}_j, \boldsymbol{\eta}_j)\|} + \sup_{\substack{(\vec{\psi}_j, \boldsymbol{\eta}_j) \in \mathbf{H}_D \\ (\vec{\psi}_j, \boldsymbol{\eta}_j) \neq \mathbf{0}}} \frac{|[c_j(\mathbf{u})(\vec{\phi}_{j,h}) - c_j(\mathbf{u}_h)(\vec{\phi}_{j,h}), \vec{\psi}_j]|}{\|(\vec{\psi}_j, \boldsymbol{\eta}_j)\|}, \end{aligned}$$

which, together with the continuity of the operator c_j (cf. [5, eq. (3.18)]), that is,

$$|[c_j(\mathbf{u})(\vec{\phi}_{j,h}) - c_j(\mathbf{u}_h)(\vec{\phi}_{j,h}), \vec{\psi}_j]| \leq \mathbf{R}_j \|\vec{\phi}_{j,h}\| \|\mathbf{u} - \mathbf{u}_h\|_{0,3;\Omega} \|\vec{\psi}_j\|,$$

where \mathbf{R}_j is a respective continuity constant, yields

$$\|(\vec{\phi}_j, \boldsymbol{\rho}_j) - (\vec{\phi}_{j,h}, \boldsymbol{\rho}_{j,h})\| \leq \frac{1}{\gamma_j} (\|\tilde{\mathcal{Q}}_j\| + \|\tilde{\mathcal{R}}_j\|) + \frac{\mathbf{R}_j}{\gamma_j} \|\vec{\phi}_{j,h}\| \|\mathbf{u} - \mathbf{u}_h\|_{0,3;\Omega}.$$

Thus, summing up over $j \in \{1, 2\}$, using the *a priori* estimate [5, eq. (4.29) in Theorem 4.10] to bound $\|\vec{\phi}_{j,h}\|$ in terms of $\|\phi_{j,D}\|_{1/2, \Gamma}$, we obtain

$$\sum_{j=1}^2 \|(\vec{\phi}_j, \boldsymbol{\rho}_j) - (\vec{\phi}_{j,h}, \boldsymbol{\rho}_{j,h})\| \leq \sum_{j=1}^2 \frac{1}{\gamma_j} (\|\tilde{\mathcal{Q}}_j\| + \|\tilde{\mathcal{R}}_j\|) + c(r) \|\phi_D\|_{1/2, \Gamma} \|\mathbf{u} - \mathbf{u}_h\|_{0,3;\Omega}, \quad (3.37)$$

where $\|\phi_D\|_{1/2,\Gamma} := \|\phi_{1,D}\|_{1/2,\Gamma} + \|\phi_{2,D}\|_{1/2,\Gamma}$ and $c(r)$ is a positive constant depending only on r and data, and hence independent of h . Finally, it is clear that (3.36) follows from (3.37), with $C_3(r) := \max\{1/\gamma_1, 1/\gamma_2, c(r)\}$, concluding the proof. \square

The derivation of our residual-based estimator will now follow from (3.22) and (3.36). In fact, bounding $\|\phi - \phi_h\|_{0,6;\Omega}$ in (3.22) by the right-hand side of (3.36), we find that

$$\begin{aligned} \|(\bar{\mathbf{u}}, \boldsymbol{\sigma}) - (\bar{\mathbf{u}}_h, \boldsymbol{\sigma}_h)\| &\leq C_1(r) \left\{ \|\mathcal{Q}\| + \|\mathcal{R}\| + \|\mathcal{R}\|^2 \right\} + C(r) \|\mathbf{g}\|_{0,\Omega} \sum_{j=1}^2 \left(\|\tilde{\mathcal{Q}}_j\| + \|\tilde{\mathcal{R}}_j\| \right) \\ &\quad + C(r) \|\mathbf{g}\|_{0,\Omega} \|\phi_D\|_{1/2,\Gamma} \|\mathbf{u} - \mathbf{u}_h\|_{0,3;\Omega}, \end{aligned} \quad (3.38)$$

where $C(r) := C_2(r) C_3(r)$. Thus, under the assumption (3.17) with this constant $C(r)$, and noting that when $\|\mathcal{R}\| < 1$ the term $\|\mathcal{R}\|^2$ is dominated by $\|\mathcal{R}\|$, whence the former can be neglected, it follows from (3.38) that

$$\|(\bar{\mathbf{u}}, \boldsymbol{\sigma}) - (\bar{\mathbf{u}}_h, \boldsymbol{\sigma}_h)\| \leq \widehat{C}(r) \left\{ \|\mathcal{Q}\| + \|\mathcal{R}\| + \sum_{j=1}^2 \left(\|\tilde{\mathcal{Q}}_j\| + \|\tilde{\mathcal{R}}_j\| \right) \right\}, \quad (3.39)$$

with $\widehat{C}(r) > 0$, independent of h . In turn, employing (3.39) to bound the last term on the right-hand side of (3.36), we derive the corresponding upper bound for $\sum_{j=1}^2 \|(\vec{\phi}_j, \boldsymbol{\rho}_j) - (\vec{\phi}_{j,h}, \boldsymbol{\rho}_{j,h})\|$. More precisely, we have proved the following result.

Lemma 3.7 *Assume (3.17) with the aforementioned constant $C(r)$. Then, there exists a positive constant C , independent of h , but depending on $r, L_{\text{BF}}, \alpha_{\text{BF}}, \beta, \|\mathbf{g}\|_{0,\Omega}, \mathbf{R}_j, j \in \{1, 2\}$, and the datum ϕ_D , such that*

$$\begin{aligned} \|(\bar{\mathbf{u}}, \boldsymbol{\sigma}) - (\bar{\mathbf{u}}_h, \boldsymbol{\sigma}_h)\| &+ \sum_{j=1}^2 \|(\vec{\phi}_j, \boldsymbol{\rho}_j) - (\vec{\phi}_{j,h}, \boldsymbol{\rho}_{j,h})\| \\ &\leq C \left\{ \|\mathcal{Q}\| + \|\mathcal{R}\| + \sum_{j=1}^2 \left(\|\tilde{\mathcal{Q}}_j\| + \|\tilde{\mathcal{R}}_j\| \right) \right\}. \end{aligned} \quad (3.40)$$

Throughout the rest of this section, we provide suitable upper bounds for each one of the terms on the right-hand side of (3.40). We begin by establishing the corresponding estimates for $\|\mathcal{Q}\|$ and $\|\tilde{\mathcal{Q}}_j\|$ (cf. (3.19) and (3.33)), which follow from straightforward applications of the Cauchy–Schwarz and Hölder inequalities. We omit further details and provide the respective bounds as follows.

Lemma 3.8 *There exist constants $C_1, C_2 > 0$, independent of h , such that*

$$\|\mathcal{Q}\| \leq C_1 \left\{ \|\boldsymbol{\sigma}_h^d - \nu \mathbf{t}_h\|_{0,\Omega} + \|\mathbf{f}(\phi_h) + \operatorname{div}(\boldsymbol{\sigma}_h) - \mathbf{K}^{-1} \mathbf{u}_h - \mathbf{F} |\mathbf{u}_h| \mathbf{u}_h\|_{0,3/2;\Omega} \right\} \quad (3.41)$$

and

$$\|\tilde{\mathcal{Q}}_j\| \leq C_2 \left\{ \|\boldsymbol{\rho}_{j,h} - \mathbf{Q}_j \tilde{\mathbf{t}}_{j,h} + \frac{1}{2} \mathbf{R}_j \phi_{j,h} \mathbf{u}_h\|_{0,\Omega} + \|\operatorname{div}(\boldsymbol{\rho}_{j,h}) - \frac{1}{2} \mathbf{R}_j \mathbf{u}_h \cdot \tilde{\mathbf{t}}_{j,h}\|_{0,6/5;\Omega} \right\}. \quad (3.42)$$

We now turn to the derivation of the corresponding estimate for $\|\mathcal{R}\|$ and $\|\tilde{\mathcal{R}}_j\|$. To that end, we first recall from (3.21) and (3.35) that $\mathcal{R}(\boldsymbol{\tau}_h) = 0$ for all $\boldsymbol{\tau}_h \in \mathbf{H}_h^\sigma$ and $\tilde{\mathcal{R}}_j(\boldsymbol{\eta}_{j,h}) = 0$ for all $\boldsymbol{\eta}_{j,h} \in \mathbf{H}_h^\rho$,

respectively, whence the aforementioned norms can be redefined as

$$\|\mathcal{R}\| := \sup_{\substack{\boldsymbol{\tau} \in \mathbb{H}_0(\mathbf{div}_{3/2}; \Omega) \\ \boldsymbol{\tau} \neq \mathbf{0}}} \frac{\mathcal{R}(\boldsymbol{\tau} - \boldsymbol{\tau}_h)}{\|\boldsymbol{\tau}\|_{\mathbf{div}_{3/2}; \Omega}} \quad \text{and} \quad \|\tilde{\mathcal{R}}_j\| := \sup_{\substack{\boldsymbol{\eta}_j \in \mathbf{H}(\mathbf{div}_{6/5}; \Omega) \\ \boldsymbol{\eta}_j \neq \mathbf{0}}} \frac{\tilde{\mathcal{R}}_j(\boldsymbol{\eta}_j - \boldsymbol{\eta}_{j,h})}{\|\boldsymbol{\eta}_j\|_{\mathbf{div}_{6/5}; \Omega}}, \quad (3.43)$$

where the functions $\boldsymbol{\tau}_h$ and $\boldsymbol{\eta}_{j,h}$ are chosen within the suprema of (3.43) so that they depend on the corresponding $\boldsymbol{\tau} \in \mathbb{H}_0(\mathbf{div}_{3/2}; \Omega)$ and $\boldsymbol{\eta}_j \in \mathbf{H}(\mathbf{div}_{6/5}; \Omega)$. More precisely, they are suitably defined in what follows by employing the Helmholtz decompositions provided by Lemma 3.2 and its tensorial version (3.10), with $p \in \{3/2, 6/5\}$. Indeed, letting $\boldsymbol{\zeta} \in \mathbb{W}^{1,3/2}(\Omega)$, $\boldsymbol{\xi} \in \mathbf{H}^1(\Omega)$, and $\zeta_j \in \mathbf{W}^{1,6/5}(\Omega)$, $\xi_j \in \mathbf{H}^1(\Omega)$, such that

$$\boldsymbol{\tau} := \boldsymbol{\zeta} + \mathbf{curl}(\boldsymbol{\xi}) \quad \text{and} \quad \boldsymbol{\eta}_j := \zeta_j + \mathbf{curl}(\xi_j) \quad \text{in } \Omega, \quad (3.44)$$

with

$$\|\boldsymbol{\zeta}\|_{1,3/2;\Omega} + \|\boldsymbol{\xi}\|_{1,\Omega} \leq C_{3/2} \|\boldsymbol{\tau}\|_{\mathbf{div}_{3/2}; \Omega} \quad \text{and} \quad \|\zeta_j\|_{1,6/5;\Omega} + \|\xi_j\|_{1,\Omega} \leq C_{6/5} \|\boldsymbol{\eta}_j\|_{\mathbf{div}_{6/5}; \Omega}, \quad (3.45)$$

we set

$$\boldsymbol{\tau}_h := \boldsymbol{\Pi}_h^k(\boldsymbol{\zeta}) + \mathbf{curl}(\mathbf{I}_h(\boldsymbol{\xi})) + c\mathbb{I} \in \mathbb{H}_h^\sigma \quad \text{and} \quad \boldsymbol{\eta}_{j,h} := \boldsymbol{\Pi}_h^k(\zeta_j) + \mathbf{curl}(\mathbf{I}_h(\xi_j)) \in \mathbf{H}_h^\rho, \quad (3.46)$$

where the constant c is chosen so that $\text{tr}(\boldsymbol{\tau}_h)$ has a null mean value, and hence $\boldsymbol{\tau}_h$ does belong to \mathbb{H}_h^σ . Note that $\boldsymbol{\tau}_h$ and $\boldsymbol{\eta}_{j,h}$ can be seen as discrete Helmholtz decompositions of $\boldsymbol{\tau}$ and $\boldsymbol{\eta}_j$, respectively. In this way, using that $\mathcal{R}(c\mathbb{I}) = 0$, and denoting

$$\hat{\boldsymbol{\zeta}} := \boldsymbol{\zeta} - \boldsymbol{\Pi}_h^k(\boldsymbol{\zeta}), \quad \hat{\boldsymbol{\xi}} := \boldsymbol{\xi} - \mathbf{I}_h(\boldsymbol{\xi}), \quad \hat{\zeta}_j := \zeta_j - \boldsymbol{\Pi}_h^k(\zeta_j), \quad \text{and} \quad \hat{\xi}_j := \xi_j - \mathbf{I}_h(\xi_j),$$

it follows from (3.44) and (3.46), that

$$\mathcal{R}(\boldsymbol{\tau}) = \mathcal{R}(\boldsymbol{\tau} - \boldsymbol{\tau}_h) = \mathcal{R}(\hat{\boldsymbol{\zeta}}) + \mathcal{R}(\mathbf{curl}(\hat{\boldsymbol{\xi}})), \quad (3.47)$$

and

$$\tilde{\mathcal{R}}_j(\boldsymbol{\eta}_j) = \tilde{\mathcal{R}}_j(\boldsymbol{\eta}_j - \boldsymbol{\eta}_{j,h}) = \tilde{\mathcal{R}}_j(\hat{\zeta}_j) + \tilde{\mathcal{R}}_j(\mathbf{curl}(\hat{\xi}_j)), \quad (3.48)$$

where, according to the definitions of \mathcal{R} and $\tilde{\mathcal{R}}_j$ (cf. (3.20), (3.34)), we find that

$$\begin{aligned} \mathcal{R}(\hat{\boldsymbol{\zeta}}) &= \int_{\Omega} \mathbf{t}_h : \hat{\boldsymbol{\zeta}} + \int_{\Omega} \mathbf{u}_h \cdot \mathbf{div}(\hat{\boldsymbol{\zeta}}) - \langle \hat{\boldsymbol{\zeta}} \mathbf{n}, \mathbf{u}_D \rangle_{\Gamma}, \\ \mathcal{R}(\mathbf{curl}(\hat{\boldsymbol{\xi}})) &= \int_{\Omega} \mathbf{t}_h : \mathbf{curl}(\hat{\boldsymbol{\xi}}) - \langle \mathbf{curl}(\hat{\boldsymbol{\xi}}) \mathbf{n}, \mathbf{u}_D \rangle_{\Gamma}, \\ \tilde{\mathcal{R}}_j(\hat{\zeta}_j) &= \int_{\Omega} \tilde{\mathbf{t}}_{j,h} \cdot \hat{\zeta}_j + \int_{\Omega} \phi_{j,h} \mathbf{div}(\hat{\zeta}_j) - \langle \hat{\zeta}_j \cdot \mathbf{n}, \phi_{j,D} \rangle_{\Gamma}, \end{aligned}$$

and

$$\tilde{\mathcal{R}}_j(\mathbf{curl}(\hat{\xi}_j)) = \int_{\Omega} \tilde{\mathbf{t}}_{j,h} \cdot \mathbf{curl}(\hat{\xi}_j) - \langle \mathbf{curl}(\hat{\xi}_j) \cdot \mathbf{n}, \phi_{j,D} \rangle_{\Gamma}.$$

The following two lemmas establish the residual upper bounds for $\|\mathcal{R}\|$ and $\|\tilde{\mathcal{R}}_j\|$ (cf. (3.43)). The corresponding proofs can be derived from a slight adaptation of [23, Lemma 3.8]. We just remark that the main tools employed are integration by parts, the Cauchy–Schwarz and Hölder inequalities, suitable boundary integration by parts formulae, namely (cf. [23, eq. (3.41) in Lemma 3.8]):

$$\langle \mathbf{curl}(\hat{\boldsymbol{\xi}}) \mathbf{n}, \mathbf{u}_D \rangle_{\Gamma} = - \langle \nabla \mathbf{u}_D \mathbf{s}, \hat{\boldsymbol{\xi}} \rangle_{\Gamma} \quad \text{and} \quad \langle \mathbf{curl}(\hat{\xi}_j) \cdot \mathbf{n}, \phi_{j,D} \rangle_{\Gamma} = - \langle \nabla \phi_{j,D} \cdot \mathbf{s}, \hat{\xi}_j \rangle_{\Gamma}, \quad (3.49)$$

the approximation properties provided by Lemmas 3.1 and 3.3, and the Helmholtz stability bounds collected in (3.45). Thus, we simply state the corresponding results as follow.

Lemma 3.9 *There exists a positive constant C , independent of h , such that*

$$\|\mathcal{R}\| \leq C \left\{ \left(\sum_{T \in \mathcal{T}_h} \tilde{\Theta}_T^2 \right)^{1/2} + \left(\sum_{T \in \mathcal{T}_h} \Theta_{4,T}^3 \right)^{1/3} \right\}, \quad (3.50)$$

where $\Theta_{4,T}^3$ is defined in (3.15), and

$$\tilde{\Theta}_T^2 := h_T^2 \|\text{rot}(\mathbf{t}_h)\|_{0,T}^2 + \sum_{e \in \mathcal{E}_h(T) \cap \mathcal{E}_h(\Omega)} h_e \|\llbracket \mathbf{t}_h \mathbf{s} \rrbracket\|_{0,e}^2 + \sum_{e \in \mathcal{E}_h(T) \cap \mathcal{E}_h(\Gamma)} h_e \|\mathbf{t}_h \mathbf{s} - \nabla_{\mathbf{U}} \mathbf{s}\|_{0,e}^2.$$

Lemma 3.10 *There exists a positive constant C , independent of h , such that*

$$\sum_{j=1}^2 \|\tilde{\mathcal{R}}_j\| \leq C \left\{ \left(\sum_{T \in \mathcal{T}_h} \hat{\Theta}_T^2 \right)^{1/2} + \left(\sum_{T \in \mathcal{T}_h} \Theta_{5,T}^6 \right)^{1/6} \right\}, \quad (3.51)$$

where $\Theta_{5,T}^6$ is defined in (3.16), and

$$\begin{aligned} \hat{\Theta}_T^2 := & \sum_{j=1}^2 \left(h_T^2 \|\text{rot}(\tilde{\mathbf{t}}_{j,h})\|_{0,T}^2 + \sum_{e \in \mathcal{E}_h(T) \cap \mathcal{E}_h(\Omega)} h_e \|\llbracket \tilde{\mathbf{t}}_{j,h} \cdot \mathbf{s} \rrbracket\|_{0,e}^2 \right. \\ & \left. + \sum_{e \in \mathcal{E}_h(T) \cap \mathcal{E}_h(\Gamma)} h_e \|\tilde{\mathbf{t}}_{j,h} \cdot \mathbf{s} - \nabla \phi_{j,D} \cdot \mathbf{s}\|_{0,e}^2 \right). \end{aligned}$$

We end this section by stressing that the reliability estimate (3.18) (cf. Theorem 3.4) is a straightforward consequence of Lemmas 3.7 – 3.10, and the definition of the global estimator Θ (cf. (3.11)).

3.3 Preliminaries for efficiency

For the efficiency analysis of Θ (cf. (3.11)), we proceed as in [2], [24], [22], [9], [3] and [23], and apply the localization technique based on bubble functions, along with inverse and discrete trace inequalities. For the former, given $T \in \mathcal{T}_h$, we let T be the usual element-bubble function (cf. [31, eqs. (1.5) and (1.6)]), which satisfies

$$\psi_T \in \mathbf{P}_3(T), \quad \text{supp}(\psi_T) \subseteq T, \quad \psi_T = 0 \quad \text{on} \quad \partial T \quad \text{and} \quad 0 \leq \psi_T \leq 1 \quad \text{in} \quad T.$$

The specific properties of ψ_T to be employed in what follows, are collected in the following lemma, for whose proof we refer to [31, Lemma 3.3 and Remark 3.2].

Lemma 3.11 *Let k be a non-negative integer, and let $p, q \in (1, +\infty)$ conjugate to each other, that is such that $1/p + 1/q = 1$, and $T \in \mathcal{T}_h$. Then, there exist positive constants c_1 , c_2 , and c_3 , independent of h and T , but depending on the shape-regularity of the triangulations (minimum angle condition) and k , such that for each $u \in \mathbf{P}_k(T)$ there hold*

$$c_1 \|u\|_{0,p;T} \leq \sup_{\substack{v \in \mathbf{P}_k(T) \\ v \neq 0}} \frac{\int_T u \psi_T v}{\|v\|_{0,q;T}} \leq \|u\|_{0,p;T},$$

and

$$c_2 h_T^{-1} \|\psi_T u\|_{0,q;T} \leq \|\nabla(\psi_T u)\|_{0,q;T} \leq c_3 h_T^{-1} \|\psi_T u\|_{0,q;T}.$$

In turn, the aforementioned inverse inequality is stated as follows (cf. [26, Lemma 1.138]).

Lemma 3.12 *Let k, l , and m be non-negative integers such that $m \leq l$, and let $r, s \in [1, +\infty]$, and $T \in \mathcal{T}_h$. Then, there exists $c > 0$, independent of h, T, r , and s , but depending on k, l, m , and the shape regularity of the triangulations, such that*

$$\|v\|_{l,r;T} \leq c h_T^{m-l+n(1/r-1/s)} \|v\|_{m,s;T} \quad \forall v \in \mathbb{P}_k(T). \quad (3.52)$$

Finally, proceeding as in [1, Theorem 3.10], that is employing the usual scaling estimates with respect to a fixed reference element \hat{T} , and applying the trace inequality in $W^{1,p}(\hat{T})$, for a given $p \in (1, +\infty)$, one is able to establish the following discrete trace inequality.

Lemma 3.13 *Let $p \in (1, +\infty)$. Then, there exists $c > 0$, depending only on the shape regularity of the triangulations, such that for each $T \in \mathcal{T}_h$ and $e \in \mathcal{E}(T)$, there holds*

$$\|v\|_{0,p;e}^p \leq c \left\{ h_T^{-1} \|v\|_{0,p;T}^p + h_T^{p-1} |v|_{1,p;T}^p \right\} \quad \forall v \in W^{1,p}(T). \quad (3.53)$$

3.4 Efficiency

We now aim to establish the efficiency estimate of Θ (cf. (3.11)). For this purpose, we will make extensive use of the original system of equations given by (2.7), which is recovered from the fully-mixed continuous formulation (2.9) by choosing suitable test functions and integrating by parts backwardly the corresponding equations. The following theorem is the main result of this section.

Theorem 3.14 *Assume, for simplicity, that \mathbf{u}_D and $\phi_{j,D}$, $j \in \{1, 2\}$, are piecewise polynomials. Then, there exists a positive constant C_{eff} , independent of h , such that*

$$C_{\text{eff}} \Theta + \text{h.o.t.} \leq \|(\bar{\mathbf{u}}, \boldsymbol{\sigma}) - (\bar{\mathbf{u}}_h, \boldsymbol{\sigma}_h)\| + \sum_{j=1}^2 \|(\vec{\phi}_j, \boldsymbol{\rho}_j) - (\vec{\phi}_{j,h}, \boldsymbol{\rho}_{j,h})\|, \quad (3.54)$$

where h.o.t. stands for one or several terms of higher order.

The proof of (3.54) is carried out throughout the rest of this section. We begin the derivation of the efficiency estimates with the following result.

Lemma 3.15 *There exist positive constants C_1, C_2, C_3 , and C_4 , independent of h , such that for each $T \in \mathcal{T}_h$ there hold*

$$\|\boldsymbol{\sigma}_h^d - \nu \mathbf{t}_h\|_{0,T} \leq C_1 \left\{ \|\boldsymbol{\sigma} - \boldsymbol{\sigma}_h\|_{0,T} + \|\mathbf{t} - \mathbf{t}_h\|_{0,T} \right\}, \quad (3.55)$$

$$\begin{aligned} & \|\mathbf{f}(\phi_h) + \text{div}(\boldsymbol{\sigma}_h) - \mathbf{K}^{-1} \mathbf{u}_h - \mathbf{F} |\mathbf{u}_h| \mathbf{u}_h\|_{0,3/2;T} \\ & \leq C_2 \left\{ \|\mathbf{u} - \mathbf{u}_h\|_{0,3;T} + \|\boldsymbol{\sigma} - \boldsymbol{\sigma}_h\|_{\text{div}_{3/2};T} + \|\phi - \phi_h\|_{0,6;T} \right\}, \end{aligned} \quad (3.56)$$

$$\begin{aligned} & \|\text{div}(\boldsymbol{\rho}_{j,h}) - \frac{1}{2} \mathbf{R}_j \mathbf{u}_h \cdot \tilde{\mathbf{t}}_{j,h}\|_{0,6/5;T} \\ & \leq C_3 \left\{ \|\mathbf{u} - \mathbf{u}_h\|_{0,3;T} + \|\tilde{\mathbf{t}}_j - \tilde{\mathbf{t}}_{j,h}\|_{0,T} + \|\boldsymbol{\rho}_j - \boldsymbol{\rho}_{j,h}\|_{\text{div}_{6/5};T} \right\}, \quad \text{and} \end{aligned} \quad (3.57)$$

$$\begin{aligned} & \|\boldsymbol{\rho}_{j,h} - \mathbf{Q}_j \tilde{\mathbf{t}}_{j,h} + \frac{1}{2} \mathbf{R}_j \phi_{j,h} \mathbf{u}_h\|_{0,T} \\ & \leq C_4 \left\{ \|\mathbf{u} - \mathbf{u}_h\|_{0,3;T} + \|\phi_j - \phi_{j,h}\|_{0,6;T} + \|\tilde{\mathbf{t}}_j - \tilde{\mathbf{t}}_{j,h}\|_{0,T} + \|\boldsymbol{\rho}_j - \boldsymbol{\rho}_{j,h}\|_{0,T} \right\}. \end{aligned} \quad (3.58)$$

Proof. First, in order to show (3.55), it suffices to recall that $\boldsymbol{\sigma}^d = \nu \mathbf{t}$ in Ω (cf. (2.7)). In turn, for the proof of (3.56), we use the identity $\mathbf{K}^{-1}\mathbf{u} + \mathbf{F}|\mathbf{u}|\mathbf{u} - \mathbf{div}(\boldsymbol{\sigma}) = \mathbf{f}(\phi)$ in Ω (cf. (2.7)), the fact that

$$\|\mathbf{f}(\phi) - \mathbf{f}(\phi_h)\|_{0,3/2;T} \leq \|\mathbf{g}\|_{0,T} \|\phi - \phi_h\|_{0,6;T},$$

which readily follows from the definition of \mathbf{f} (cf. (2.3)), and the Hölder inequality, to obtain

$$\begin{aligned} & \|\mathbf{f}(\phi_h) + \mathbf{div}(\boldsymbol{\sigma}_h) - \mathbf{K}^{-1}\mathbf{u}_h - \mathbf{F}|\mathbf{u}_h|\mathbf{u}_h\|_{0,3/2;T} \\ & \leq C \left\{ \|\mathbf{u} - \mathbf{u}_h\|_{0,3;T} + \|\mathbf{u}|\mathbf{u} - |\mathbf{u}_h|\mathbf{u}_h\|_{0,3/2;T} + \|\boldsymbol{\sigma} - \boldsymbol{\sigma}_h\|_{\mathbf{div}_{3/2};T} + \|\phi - \phi_h\|_{0,6;T} \right\}, \end{aligned} \quad (3.59)$$

where C is a positive constant depending only on $\|\mathbf{g}\|_{0,T}$, \mathbf{K} , and \mathbf{F} . Next, adding and subtracting $|\mathbf{u}|\mathbf{u}_h$ (also work with $|\mathbf{u}_h|\mathbf{u}$), and employing the triangle and Cauchy–Schwarz inequalities, we find that

$$\|\mathbf{u}|\mathbf{u} - |\mathbf{u}_h|\mathbf{u}_h\|_{0,3/2;T} \leq (\|\mathbf{u}\|_{0,3;T} + \|\mathbf{u}_h\|_{0,3;T})\|\mathbf{u} - \mathbf{u}_h\|_{0,3;T},$$

which, together with the fact that $\|\mathbf{u}\|_{0,3;T}$ and $\|\mathbf{u}_h\|_{0,3;T}$ are bounded by $\|\mathbf{u}\|_{0,3;\Omega}$ and $\|\mathbf{u}_h\|_{0,3;\Omega}$, respectively, which in turn are bounded by data (cf. [5, eqs. (3.50) and (4.27)]), allows us to deduce that there exists a positive constant C , independent of h , such that

$$\|\mathbf{u}|\mathbf{u} - |\mathbf{u}_h|\mathbf{u}_h\|_{0,3/2;T} \leq C \|\mathbf{u} - \mathbf{u}_h\|_{0,3;T}. \quad (3.60)$$

Then, replacing (3.60) back into (3.59), we conclude (3.56). On the other hand, the proof of (3.57) and (3.58), follow from a slight adaptation of [23, eqs. (3.51) and (3.52) in Lemma 3.14], respectively. We just observe here that the main tools used are the identities $\mathbf{Q}_j \tilde{\mathbf{t}}_j - \frac{1}{2} \mathbf{R}_j \phi_j \mathbf{u} = \boldsymbol{\rho}_j$ and $\frac{1}{2} \mathbf{R}_j \mathbf{u} \cdot \tilde{\mathbf{t}}_j - \mathbf{div}(\boldsymbol{\rho}_j) = 0$ in Ω (cf. (2.7)), the triangle and Hölder inequalities, the estimates

$$\|\mathbf{u} \cdot \tilde{\mathbf{t}}_j - \mathbf{u}_h \cdot \tilde{\mathbf{t}}_{j,h}\|_{0,6/5;T} \leq (\|\mathbf{u}_h\|_{0,3;T} + \|\tilde{\mathbf{t}}_j\|_{0,T}) (\|\mathbf{u} - \mathbf{u}_h\|_{0,3;T} + \|\tilde{\mathbf{t}}_j - \tilde{\mathbf{t}}_{j,h}\|_{0,T}),$$

and

$$\|\phi_j \mathbf{u} - \phi_{j,h} \mathbf{u}_h\|_{0,T} \leq (\|\mathbf{u}_h\|_{0,3;T} + \|\phi_j\|_{0,6;T}) (\|\mathbf{u} - \mathbf{u}_h\|_{0,3;T} + \|\phi_j - \phi_{j,h}\|_{0,6;T}),$$

and, similarly to (3.60), the fact that $\|\phi_j\|_{0,6;T}$, $\|\tilde{\mathbf{t}}_j\|_{0,T}$, and $\|\mathbf{u}_h\|_{0,3;T}$ are bounded by $\|\phi_j\|_{0,6;\Omega}$, $\|\tilde{\mathbf{t}}_j\|_{0,\Omega}$, and $\|\mathbf{u}_h\|_{0,3;\Omega}$, respectively, which in turn are bounded by data (cf. [5, eqs. (3.52), (4.27)]). Further details are omitted. \square

At this point, we stress that the local efficiency estimates for the remaining terms defining Θ (cf. (3.11)) have already been proved in the literature by using the localization technique based on triangle-bubble and edge-bubble functions (cf. Lemma 3.11), the local inverse inequality (cf. (3.52)), and the discrete trace inequality (cf. (3.53)). More precisely, we provide the following result.

Lemma 3.16 *Assume that \mathbf{u}_D and $\phi_{j,D}$, $j \in \{1, 2\}$, are piecewise polynomials. Then, there exist positive constants C_i , $i \in \{1, \dots, 10\}$, all independent of h , such that*

- a) $h_T^3 \|\mathbf{t}_h - \nabla \mathbf{u}_h\|_{0,3;T}^3 \leq C_1 \left\{ \|\mathbf{u} - \mathbf{u}_h\|_{0,3;T}^3 + h_T \|\mathbf{t} - \mathbf{t}_h\|_{0,T}^3 \right\} \quad \forall T \in \mathcal{T}_h,$
- b) $h_T^6 \|\tilde{\mathbf{t}}_{j,h} - \nabla \phi_{j,h}\|_{0,6;T}^6 \leq C_2 \left\{ \|\phi_j - \phi_{j,h}\|_{0,6;T}^6 + h_T \|\tilde{\mathbf{t}}_j - \tilde{\mathbf{t}}_{j,h}\|_{0,T}^6 \right\} \quad \forall T \in \mathcal{T}_h,$
- c) $h_e \|\mathbf{u}_D - \mathbf{u}_h\|_{0,3;e}^3 \leq C_3 \left\{ \|\mathbf{u} - \mathbf{u}_h\|_{0,3;T_e}^3 + h_{T_e} \|\mathbf{t} - \mathbf{t}_h\|_{0,T_e}^3 \right\} \quad \forall e \in \mathcal{E}_h(\Gamma),$
- d) $h_e \|\phi_{j,D} - \phi_{j,h}\|_{0,6;e}^6 \leq C_4 \left\{ \|\phi_j - \phi_{j,h}\|_{0,6;T_e}^6 + h_{T_e} \|\tilde{\mathbf{t}}_j - \tilde{\mathbf{t}}_{j,h}\|_{0,T_e}^6 \right\} \quad \forall e \in \mathcal{E}_h(\Gamma),$

- e) $h_T^2 \|\text{rot}(\mathbf{t}_h)\|_{0,T}^2 \leq C_5 \|\mathbf{t} - \mathbf{t}_h\|_{0,T}^2 \quad \forall T \in \mathcal{T}_h,$
- f) $h_T^2 \|\text{rot}(\tilde{\mathbf{t}}_{j,h})\|_{0,T}^2 \leq C_6 \|\tilde{\mathbf{t}}_j - \tilde{\mathbf{t}}_{j,h}\|_{0,T}^2 \quad \forall T \in \mathcal{T}_h,$
- g) $h_e \|\llbracket \mathbf{t}_h \mathbf{s} \rrbracket\|_{0,e}^2 \leq C_7 \|\mathbf{t} - \mathbf{t}_h\|_{0,\omega_e}^2 \quad \forall e \in \mathcal{E}_h(\Omega),$
- h) $h_e \|\llbracket \tilde{\mathbf{t}}_{j,h} \mathbf{s} \rrbracket\|_{0,e}^2 \leq C_8 \|\tilde{\mathbf{t}}_j - \tilde{\mathbf{t}}_{j,h}\|_{0,\omega_e}^2 \quad \forall e \in \mathcal{E}_h(\Omega),$
- i) $h_e \|\mathbf{t}_\mathbf{s} - \nabla \mathbf{u}_\mathbf{s}\|_{0,e}^2 \leq C_9 \|\mathbf{t} - \mathbf{t}_h\|_{0,T_e}^2 \quad \forall e \in \mathcal{E}_h(\Gamma),$
- j) $h_e \|\tilde{\mathbf{t}}_{j,h} \cdot \mathbf{s} - \nabla \phi_{j,D} \cdot \mathbf{s}\|_{0,e}^2 \leq C_{10} \|\tilde{\mathbf{t}}_j - \tilde{\mathbf{t}}_{j,h}\|_{0,T_e}^2 \quad \forall e \in \mathcal{E}_h(\Gamma),$

where T_e is the triangle of \mathcal{T}_h having e as an edge, whereas ω_e denotes the union of the two elements of \mathcal{T}_h sharing the edge e .

Proof. The estimates a) and b) follow straightforwardly from a slight modification of the proof of [23, Lemma 3.17], whereas c) and d) follow from [23, Lemma 3.18]. In turn, for the proof of e), f), g) and h), we refer to [2, Lemmas 4.3 and 4.4]. Finally, the proof of i) and j) follow the same arguments to the ones used in the proof of [24, Lemma 4.15]. \square

We note here that if \mathbf{u}_D and $\phi_{j,D}$, $j \in \{1, 2\}$ were not piecewise polynomials but sufficiently smooth, then higher order terms given by the errors arising from suitable polynomial approximations of these expressions and functions would appear in the efficiency estimates c), d), i), and j), provided in Lemma 3.16, which explains the expression h.o.t. in the lower bound of (3.54).

We end this section by observing that the proof of (3.54) (cf. Theorem 3.14) follows straightforwardly from Lemmas 3.15 and 3.16, and after summing up the local efficiency estimates over all $T \in \mathcal{T}_h$. Further details are omitted.

4 A posteriori error analysis: The 3D case

In this section we extend the results from Section 3 to the three-dimensional version of (2.18). Similarly as in the previous section, given a tetrahedron $T \in \mathcal{T}_h$, we let $\mathcal{E}(T)$ be the set of its faces, and let \mathcal{E}_h be the set of all faces of the triangulation \mathcal{T}_h . Then, we write $\mathcal{E}_h = \mathcal{E}_h(\Omega) \cup \mathcal{E}_h(\Gamma)$, where $\mathcal{E}_h(\Omega) := \{e \in \mathcal{E}_h : e \subseteq \Omega\}$ and $\mathcal{E}_h(\Gamma) := \{e \in \mathcal{E}_h : e \subseteq \Gamma\}$. Also, for each face $e \in \mathcal{E}_h$ we fix a unit normal vector \mathbf{n}_e to e , and then, given $\mathbf{v} = (v_1, v_2, v_3)^t \in \mathbf{L}^2(\Omega)$ and $\boldsymbol{\tau} := (\tau_{i,j})_{3 \times 3} \in \mathbb{L}^2(\Omega)$ such that $\mathbf{v}|_T \in \mathbf{C}(T)$ and $\boldsymbol{\tau}|_T \in \mathbb{C}(T)$ on each $T \in \mathcal{T}_h$, we let $\llbracket \mathbf{v} \times \mathbf{n}_e \rrbracket$ and $\llbracket \boldsymbol{\tau} \times \mathbf{n}_e \rrbracket$ be the corresponding jumps of the tangential traces across e . In other words, $\llbracket \mathbf{v} \times \mathbf{n}_e \rrbracket = (\mathbf{v}|_T - \mathbf{v}|_{T'}) \times \mathbf{n}_e$ and $\llbracket \boldsymbol{\tau} \times \mathbf{n}_e \rrbracket = (\boldsymbol{\tau}|_T - \boldsymbol{\tau}|_{T'}) \times \mathbf{n}_e$, respectively, where T and T' are the tetrahedron of \mathcal{T}_h having e as a common face and

$$\boldsymbol{\tau} \times \mathbf{n}_e := \begin{pmatrix} (\tau_{11}, \tau_{12}, \tau_{13}) \times \mathbf{n}_e \\ (\tau_{21}, \tau_{22}, \tau_{23}) \times \mathbf{n}_e \\ (\tau_{31}, \tau_{32}, \tau_{33}) \times \mathbf{n}_e \end{pmatrix}.$$

From now on, when no confusion arises, we simply write \mathbf{n} instead of \mathbf{n}_e . In the sequel we will also make use of the following differential operators

$$\mathbf{curl}(\mathbf{v}) = \nabla \times \mathbf{v} := \left(\frac{\partial v_3}{\partial x_2} - \frac{\partial v_2}{\partial x_3}, \frac{\partial v_1}{\partial x_3} - \frac{\partial v_3}{\partial x_1}, \frac{\partial v_2}{\partial x_1} - \frac{\partial v_1}{\partial x_2} \right),$$

and

$$\underline{\mathbf{curl}}(\boldsymbol{\tau}) := \begin{pmatrix} \mathbf{curl}(\tau_{11}, \tau_{12}, \tau_{13}) \\ \mathbf{curl}(\tau_{21}, \tau_{22}, \tau_{23}) \\ \mathbf{curl}(\tau_{31}, \tau_{32}, \tau_{33}) \end{pmatrix}.$$

In turn, the tangential curl operator \mathbf{curl}_s and a tensor version of it, denoted $\underline{\mathbf{curl}}_s$, which is defined component-wise by \mathbf{curl}_s , will also be used (see [6, Section 3] for details).

We now set for each $T \in \mathcal{T}_h$

$$\begin{aligned}
\Theta_{3,T}^2 &:= \|\boldsymbol{\sigma}_h^d - \nu \mathbf{t}_h\|_{0,T}^2 + h_T^2 \|\underline{\mathbf{curl}}(\mathbf{t}_h)\|_{0,T}^2 \\
&+ \sum_{e \in \mathcal{E}_h(T) \cap \mathcal{E}_h(\Omega)} h_e \|\llbracket \mathbf{t}_h \times \mathbf{n} \rrbracket\|_{0,e}^2 + \sum_{e \in \mathcal{E}_h(T) \cap \mathcal{E}_h(\Gamma)} h_e \|\mathbf{t}_h \times \mathbf{n} - \underline{\mathbf{curl}}_s(\mathbf{u}_D)\|_{0,e}^2 \\
&+ \sum_{j=1}^2 \left(\|\boldsymbol{\rho}_{j,h} - \mathbf{Q}_j \tilde{\mathbf{t}}_{j,h} + \frac{1}{2} \mathbf{R}_j \phi_{j,h} \mathbf{u}_h\|_{0,T}^2 + h_T^2 \|\mathbf{curl}(\tilde{\mathbf{t}}_{j,h})\|_{0,T}^2 \right. \\
&\left. + \sum_{e \in \mathcal{E}_h(T) \cap \mathcal{E}_h(\Omega)} h_e \|\llbracket \tilde{\mathbf{t}}_{j,h} \times \mathbf{n} \rrbracket\|_{0,e}^2 + \sum_{e \in \mathcal{E}_h(T) \cap \mathcal{E}_h(\Gamma)} h_e \|\tilde{\mathbf{t}}_{j,h} \times \mathbf{n} - \underline{\mathbf{curl}}_s(\phi_{j,D})\|_{0,e}^2 \right),
\end{aligned} \tag{4.1}$$

and the global *a posteriori* error estimator is defined as

$$\begin{aligned}
\Theta &= \left\{ \sum_{T \in \mathcal{T}_h} \Theta_{1,T}^{6/5} \right\}^{5/6} + \left\{ \sum_{T \in \mathcal{T}_h} \Theta_{2,T}^{3/2} \right\}^{2/3} + \left\{ \sum_{T \in \mathcal{T}_h} \Theta_{3,T}^2 \right\}^{1/2} \\
&+ \left\{ \sum_{T \in \mathcal{T}_h} \Theta_{4,T}^3 \right\}^{1/3} + \left\{ \sum_{T \in \mathcal{T}_h} \Theta_{5,T}^6 \right\}^{1/6},
\end{aligned} \tag{4.2}$$

where $\Theta_{1,T}^{6/5}$, $\Theta_{2,T}^{3/2}$, $\Theta_{4,T}^3$, and $\Theta_{5,T}^6$ are defined as in (3.12), (3.13), (3.15), and (3.16), respectively. In this way, the corresponding reliability and efficiency estimates, which constitute the analogue of Theorems 3.4 and 3.14, are stated as follows.

Theorem 4.1 *Assume (3.17) and that \mathbf{u}_D and ϕ_D are piecewise polynomials. Then, there exist positive constants C_{real} and C_{eff} , independent of h , such that*

$$C_{\text{eff}} \Theta + \text{h.o.t.} \leq \|(\bar{\mathbf{u}}, \boldsymbol{\sigma}) - (\bar{\mathbf{u}}_h, \boldsymbol{\sigma}_h)\| + \sum_{j=1}^2 \|(\vec{\phi}_j, \boldsymbol{\rho}_j) - (\vec{\phi}_{j,h}, \boldsymbol{\rho}_{j,h})\| \leq C_{\text{real}} \Theta.$$

The proof of Theorem 4.1 follows very closely the analysis of Section 3, except a few issues to be described throughout the following discussion. Indeed, we first notice that the general *a posteriori* error estimate given by Lemma 3.7 and the upper bounds for $\|\mathcal{Q}\|$ and $\|\tilde{\mathcal{Q}}_j\|$ (cf. (3.41), (3.42)), are also valid in 3D. In turn, we follow [20, Theorem 3.2] to derive a 3D version for arbitrary polyhedral domains of the Helmholtz decomposition provided by Lemma 3.2, with $p \geq 6/5$ (cf. [3, Lemma 3.4]). Next, the associated discrete Helmholtz decomposition and the functionals \mathcal{R} and $\tilde{\mathcal{R}}_j$ are set and rewritten exactly as in (3.46), (3.47), and (3.48), respectively. In addition, in order to derive the new upper bounds of $\|\mathcal{R}\|$ and $\|\tilde{\mathcal{R}}_j\|$ (cf. (3.43)), we now need the 3D analogue of the integration by parts formulae on the boundary given by (3.49). In fact, by employing the identities from [26, Chapter I, eq. (2.17), and Theorem 2.11], we deduce that in this case there holds

$$\langle \mathbf{curl}(\boldsymbol{\xi}) \cdot \mathbf{n}, \theta \rangle_\Gamma = - \langle \mathbf{curl}_s(\theta), \boldsymbol{\xi} \rangle_\Gamma \quad \forall \boldsymbol{\xi} \in \mathbf{H}^1(\Omega), \quad \forall \theta \in H^{1/2}(\Gamma).$$

In addition, the integration by parts formula on each tetrahedron $T \in \mathcal{T}_h$, which is used in the proof of the 3D analogues of Lemmas 3.9 and 3.10, becomes (cf. [26, Chapter I, Theorem 2.11])

$$\int_T \mathbf{curl}(\mathbf{q}) \cdot \boldsymbol{\xi} - \int_T \mathbf{q} \cdot \mathbf{curl}(\boldsymbol{\xi}) = \langle \mathbf{q} \times \mathbf{n}, \boldsymbol{\xi} \rangle_{\partial T} \quad \forall \mathbf{q} \in \mathbf{H}(\mathbf{curl}; \Omega), \quad \forall \boldsymbol{\xi} \in \mathbf{H}^1(\Omega),$$

where $\langle \cdot, \cdot \rangle_{\partial T}$ is the duality pairing between $\mathbf{H}^{-1/2}(\partial T)$ and $\mathbf{H}^{1/2}(\partial T)$, and, as usual, $\mathbf{H}(\mathbf{curl}; \Omega)$ is the space of vectors in $\mathbf{L}^2(\Omega)$ whose \mathbf{curl} belongs to $\mathbf{L}^2(\Omega)$. We observe that, unlike the 2D case, it is not necessary for the reliability analysis to assume that $\mathbf{u}_D \in \mathbf{H}^1(\Gamma)$ and $\phi_{j,D} \in \mathbf{H}^1(\Gamma)$, $j \in \{1, 2\}$, since the \mathbf{curl}_s is defined into $\mathbf{H}^{1/2}(\Gamma)$. Nevertheless, for computational purposes, in Section 5 we will consider that \mathbf{u}_D and $\phi_{j,D}$ are sufficiently smooth, in which case $\underline{\mathbf{curl}}_s(\mathbf{u}_D)$ (resp. $\mathbf{curl}_s(\phi_{j,D})$) coincides with $\nabla \mathbf{u}_D \times \mathbf{n}$ (resp. $\nabla \phi_{j,D} \times \mathbf{n}$).

Finally, in order to prove the efficiency of Θ (cf. (4.2)), we first observe that the terms defining $\Theta_{1,T}^{6/5}$, $\Theta_{2,T}^{3/2}$, and the first and fifth terms defining $\Theta_{3,T}^2$ (cf. (3.12), (3.13), (3.14)), are estimated exactly as done for the 2D case in Lemma 3.15. For the remaining terms, we establish the following lemma.

Lemma 4.2 *Assume that \mathbf{u}_D and $\phi_{j,D}$, $j \in \{1, 2\}$, are piecewise polynomials. Then, there exist positive constants \widehat{C}_i , $i \in \{1, \dots, 10\}$, all independent of h , such that*

- a) $h_T^3 \|\mathbf{t}_h - \nabla \mathbf{u}_h\|_{0,3;T}^3 \leq \widehat{C}_1 \left\{ \|\mathbf{u} - \mathbf{u}_h\|_{0,3;T}^3 + h_T \|\mathbf{t} - \mathbf{t}_h\|_{0,T}^3 \right\} \quad \forall T \in \mathcal{T}_h,$
- b) $h_T^6 \|\widetilde{\mathbf{t}}_{j,h} - \nabla \phi_{j,h}\|_{0,6;T}^6 \leq \widehat{C}_2 \left\{ \|\phi_j - \phi_{j,h}\|_{0,6;T}^6 + h_T \|\widetilde{\mathbf{t}}_j - \widetilde{\mathbf{t}}_{j,h}\|_{0,T}^6 \right\} \quad \forall T \in \mathcal{T}_h,$
- c) $h_e \|\mathbf{u}_D - \mathbf{u}_h\|_{0,3;e}^3 \leq \widehat{C}_3 \left\{ \|\mathbf{u} - \mathbf{u}_h\|_{0,3;T_e}^3 + h_{T_e} \|\mathbf{t} - \mathbf{t}_h\|_{0,T_e}^3 \right\} \quad \forall e \in \mathcal{E}_h(\Gamma),$
- d) $h_e \|\phi_{j,D} - \phi_{j,h}\|_{0,6;e}^6 \leq \widehat{C}_4 \left\{ \|\phi_j - \phi_{j,h}\|_{0,6;T_e}^6 + h_{T_e} \|\widetilde{\mathbf{t}}_j - \widetilde{\mathbf{t}}_{j,h}\|_{0,T_e}^6 \right\} \quad \forall e \in \mathcal{E}_h(\Gamma).$
- e) $h_T^2 \|\underline{\mathbf{curl}}(\mathbf{t}_h)\|_{0,T}^2 \leq \widehat{C}_5 \|\mathbf{t} - \mathbf{t}_h\|_{0,T}^2 \quad \forall T \in \mathcal{T}_h,$
- f) $h_T^2 \|\underline{\mathbf{curl}}(\widetilde{\mathbf{t}}_{j,h})\|_{0,T}^2 \leq \widehat{C}_6 \|\widetilde{\mathbf{t}}_j - \widetilde{\mathbf{t}}_{j,h}\|_{0,T}^2 \quad \forall T \in \mathcal{T}_h,$
- g) $h_e \|\llbracket \mathbf{t}_h \times \mathbf{n} \rrbracket\|_{0,e}^2 \leq \widehat{C}_7 \|\mathbf{t} - \mathbf{t}_h\|_{0,\omega_e}^2 \quad \forall e \in \mathcal{E}_h(\Omega),$
- h) $h_e \|\llbracket \widetilde{\mathbf{t}}_{j,h} \times \mathbf{n} \rrbracket\|_{0,e}^2 \leq \widehat{C}_8 \|\widetilde{\mathbf{t}}_j - \widetilde{\mathbf{t}}_{j,h}\|_{0,\omega_e}^2 \quad \forall e \in \mathcal{E}_h(\Omega),$
- i) $h_e \|\mathbf{t}_h \times \mathbf{n} - \underline{\mathbf{curl}}_s(\mathbf{u}_D)\|_{0,e}^2 \leq \widehat{C}_9 \|\mathbf{t} - \mathbf{t}_h\|_{0,T_e}^2 \quad \forall e \in \mathcal{E}_h(\Gamma),$
- j) $h_e \|\widetilde{\mathbf{t}}_{j,h} \times \mathbf{n} - \mathbf{curl}_s(\phi_{j,D})\|_{0,e}^2 \leq \widehat{C}_{10} \|\widetilde{\mathbf{t}}_j - \widetilde{\mathbf{t}}_{j,h}\|_{0,T_e}^2 \quad \forall e \in \mathcal{E}_h(\Gamma).$

Proof. For a) and b) we refer again to [23, Lemma 3.17] by using now the local inverse inequality (3.52) with $n = 3$, whereas c) and d) follow from [23, Lemma 3.18] and the present estimates a) and b). In turn, for the proof of e), f), g) and h), we refer to [22, Lemmas 4.9 and 4.10]. Finally, i) and j) can be derived after slight modification of the proof of [24, Lemma 4.15], along with the definitions of $\underline{\mathbf{curl}}_s$ and \mathbf{curl}_s , respectively. \square

5 Numerical results

This section serves to illustrate the performance and accuracy of the proposed fully-mixed finite element scheme (2.18) along with the reliability and efficiency properties of the *a posteriori* error estimator Θ (cf. (3.11)), in 2D and 3D domains. In what follows, we refer to the corresponding sets of finite element subspaces generated by $k = 0$ and $k = 1$, as simply $\mathbf{P}_0 - \mathbb{P}_0 - \mathbf{RT}_0 - \mathbf{P}_0 - \mathbf{P}_0 - \mathbf{RT}_0$ and $\mathbf{P}_1 - \mathbb{P}_1 - \mathbf{RT}_1 - \mathbf{P}_1 - \mathbf{P}_1 - \mathbf{RT}_1$, respectively. Our implementation is based on a `FreeFem++` code [27]. Regarding the implementation of the Newton iterative method associated to (2.18) (see [5,

Section 5] for details), the iterations are terminated once the relative error of the entire coefficient vectors between two consecutive iterates, say \mathbf{coeff}^{m+1} and \mathbf{coeff}^m , is sufficiently small, that is,

$$\frac{\|\mathbf{coeff}^{m+1} - \mathbf{coeff}^m\|}{\|\mathbf{coeff}^{m+1}\|} \leq \text{tol},$$

where $\|\cdot\|$ stands for the usual Euclidean norm in \mathbb{R}^{DOF} , with DOF denoting the total number of degrees of freedom defining the finite element subspaces $\mathbf{H}_h^{\mathbf{u}}$, $\mathbb{H}_h^{\mathbf{t}}$, \mathbb{H}_h^{σ} , \mathbb{H}_h^{ϕ} , $\mathbf{H}_h^{\tilde{\mathbf{t}}}$, and \mathbf{H}_h^{ρ} (cf. (2.17)), and tol is a fixed tolerance chosen as $\text{tol} = 1\text{E} - 6$. As usual, the individual errors are denoted by:

$$\begin{aligned} \mathbf{e}(\mathbf{u}) &:= \|\mathbf{u} - \mathbf{u}_h\|_{0,3;\Omega}, & \mathbf{e}(\mathbf{t}) &:= \|\mathbf{t} - \mathbf{t}_h\|_{0,\Omega}, & \mathbf{e}(\boldsymbol{\sigma}) &:= \|\boldsymbol{\sigma} - \boldsymbol{\sigma}_h\|_{\text{div}_{3/2};\Omega}, & \mathbf{e}(p) &:= \|p - p_h\|_{0,\Omega}, \\ \mathbf{e}(\boldsymbol{\phi}) &:= \sum_{j=1}^2 \|\phi_j - \phi_{j,h}\|_{0,6;\Omega}, & \mathbf{e}(\tilde{\mathbf{t}}) &:= \sum_{j=1}^2 \|\tilde{\mathbf{t}}_j - \tilde{\mathbf{t}}_{j,h}\|_{0,\Omega}, & \mathbf{e}(\boldsymbol{\rho}) &:= \sum_{j=1}^2 \|\boldsymbol{\rho}_j - \boldsymbol{\rho}_{j,h}\|_{\text{div}_{6/5};\Omega}, \end{aligned}$$

where p_h is the post-processed pressure suggested by (2.6):

$$p_h = -\frac{1}{n} \text{tr}(\boldsymbol{\sigma}_h).$$

In turn, the global error and the effectivity index associated to the global estimator Θ are denoted, respectively, by

$$\mathbf{e}(\vec{\boldsymbol{\sigma}}) := \mathbf{e}(\mathbf{u}) + \mathbf{e}(\mathbf{t}) + \mathbf{e}(\boldsymbol{\sigma}) + \mathbf{e}(\boldsymbol{\phi}) + \mathbf{e}(\tilde{\mathbf{t}}) + \mathbf{e}(\boldsymbol{\rho}) \quad \text{and} \quad \text{eff}(\Theta) := \frac{\mathbf{e}(\vec{\boldsymbol{\sigma}})}{\Theta}.$$

Moreover, using the fact that $\text{DOF}^{-1/n} \cong h$, the respective experimental rates of convergence are computed as

$$r(\star) := -n \frac{\log(\mathbf{e}(\star)/\mathbf{e}'(\star))}{\log(\text{DOF}/\text{DOF}')} \quad \text{for each } \star \in \{\mathbf{u}, \mathbf{t}, \boldsymbol{\sigma}, p, \boldsymbol{\phi}, \tilde{\mathbf{t}}, \boldsymbol{\rho}, \vec{\boldsymbol{\sigma}}\},$$

where DOF and DOF' denote the total degrees of freedom associated to two consecutive triangulations with errors $\mathbf{e}(\star)$ and $\mathbf{e}'(\star)$, respectively.

The examples to be considered in this section are described next. In all of them, for sake of simplicity, we take $\nu = 1$, $\varrho = 1$, $\mathbf{R}_1 = 1$, $\mathbf{R}_2 = 1$, $\boldsymbol{\phi}_{\mathbf{r}} = \mathbf{0}$, $\mathbf{g} = (0, -1)^t$ when $n = 2$ and $\mathbf{g} = (0, 0, -1)^t$ when $n = 3$. In turn, in the first three examples we consider $\mathbf{F} = 10$ and the tensors \mathbf{K} , \mathbf{Q}_1 , and \mathbf{Q}_2 are taken as the identity matrix \mathbb{I} , which satisfy (2.4). Furthermore, the condition $\int_{\Omega} \text{tr}(\boldsymbol{\sigma}_h) = 0$ is imposed via a penalization strategy. Example 1 is used to show the accuracy of the method and the behaviour of the effectivity indexes of the *a posteriori* error estimator Θ , whereas Examples 2–3 and 4 are utilized to illustrate the associated adaptive algorithm, with and without manufactured solutions, respectively, in both 2D and 3D domains. The corresponding adaptivity procedure, taken from [31], is described as follows:

1. Start with a coarse mesh \mathcal{T}_h .
2. Solve the Newton iterative method associated to (2.18) for the current mesh \mathcal{T}_h .
3. Compute the local indicator $\widehat{\Theta}_T$ for each $T \in \mathcal{T}_h$, where

$$\widehat{\Theta}_T := \sum_{i=1}^5 \Theta_{i,T}. \quad (\text{cf. (3.12)–(3.16)})$$

4. Check the stopping criterion and decide whether to finish or go to next step.
5. Generate an adapted mesh through a variable metric/Delaunay automatic meshing algorithm (see [28, Section 9.1.9]).
6. Define resulting mesh as current mesh \mathcal{T}_h , and go to step (2).

Example 1: Accuracy assessment with a smooth solution in a square domain.

We first concentrate on the accuracy of the fully-mixed method as well as the properties of the *a posteriori* error estimator through the effectivity index $\mathbf{eff}(\Theta)$, under a quasi-uniform refinement strategy. We consider the square domain $\Omega = (-1, 1)^2$, and adjust the data in (2.3) so that the exact solution is given by the smooth functions

$$\mathbf{u}(x_1, x_2) = \begin{pmatrix} -\sin^2(\pi x_1) \sin(2\pi x_2) \\ \sin(2\pi x_1) \sin^2(\pi x_2) \end{pmatrix}, \quad p(x_1, x_2) = \cos(\pi x_1) \exp(x_2),$$

$$\phi_1(x_1, x_2) = 15 - 15 \exp(-x_1 x_2 (x_1 - 1)(x_2 - 1)), \quad \text{and} \quad \phi_2(x_1, x_2) = -0.5 + \exp(-x_1^2 - x_2^2).$$

Tables 5.1 and 5.2 show the convergence history for a sequence of quasi-uniform mesh refinements, including the average number of Newton iterations. The results illustrate that the optimal rates of convergence $\mathcal{O}(h^{k+1})$ established in [5, Theorem 5.5] are attained for $k = 0, 1$. In addition, the global *a posteriori* error indicator Θ (cf. (3.11)), and its respective effectivity index are also displayed there, from where we highlight that the latter remain always bounded.

Example 2: Adaptivity in a 2D L-shaped domain.

We now aim at testing the features of adaptive mesh refinement after the *a posteriori* error estimator Θ (cf. (3.11)). We consider an L-shaped domain $\Omega := (-1, 1)^2 \setminus (0, 1)^2$. The manufactured solution is given by

$$\mathbf{u}(x_1, x_2) = \begin{pmatrix} -\pi \cos(\pi x_2) \sin(\pi x_1) \\ \pi \cos(\pi x_1) \sin(\pi x_2) \end{pmatrix}, \quad p(x_1, x_2) = \frac{10(1 - x_1)}{(x_1 - 0.02)^2 + (x_2 - 0.02)^2} - p_0,$$

$$\phi_1(x_1, x_2) = \frac{1}{x_2 + 1.055}, \quad \text{and} \quad \phi_2(x_1, x_2) = \frac{1}{x_2 + 1.07},$$

where $p_0 \in \mathbb{R}$ is chosen so that $\int_{\Omega} p = 0$. Observe that the pressure, temperature and concentration fields exhibit high gradients near the vertex (0,0) and the lines $x_2 = -1.055$ and $x_2 = -1.07$, respectively. Tables 5.3–5.6 along with Figure 5.1, summarizes the convergence history of the method applied to a sequence of quasi-uniformly and adaptively refined triangulation of the domain. Suboptimal rates are observed in the first case, whereas adaptive refinement according to the *a posteriori* error indicator Θ yields optimal convergence and stable effectivity indexes. Notice how the adaptive algorithms improves the efficiency of the method by delivering quality solutions at a lower computational cost, to the point that it is possible to get a better one (in terms of $\mathbf{e}(\vec{\sigma})$) with approximately only the 0.7% of the degrees of freedom of the last quasi-uniform mesh for the fully-mixed scheme in both cases $k = 0$ and $k = 1$. Furthermore, the initial mesh and approximate solutions builded using the $\mathbf{P}_1 - \mathbb{P}_1 - \mathbb{RT}_1 - \mathbf{P}_1 - \mathbf{P}_1 - \mathbf{RT}_1$ scheme (via the indicator Θ) with 55,299 triangle elements (actually representing 2,935,459 DOF), are shown in Figure 5.2. In particular, we observe that the pressure and concentration exhibit high gradients near the contraction region and at the bottom boundary of the

L-shape domain, respectively. In turn, examples of some adapted meshes for $k = 0$ and $k = 1$ are collected in Figure 5.3. We can observe a clear clustering of elements near the corner region of the contraction and the bottom of the L-shape domain as we expected.

Example 3: Adaptivity in a 3D L-shape domain.

Here we replicate the Example 2 in a three-dimensional setting by considering the 3D L-shape domain $\Omega := (-0.5, 0.5) \times (0, 0.5) \times (-0.5, 0.5) \setminus (0, 0.5)^3$, and the manufactured exact solution

$$\mathbf{u}(x_1, x_2, x_3) = \begin{pmatrix} \sin(\pi x_1) \cos(\pi x_2) \cos(\pi x_3) \\ -2 \cos(\pi x_1) \sin(\pi x_2) \cos(\pi x_3) \\ \cos(\pi x_1) \cos(\pi x_2) \sin(\pi x_3) \end{pmatrix}, \quad p(x_1, x_2, x_3) = \frac{10x_3}{(x_1 - 0.02)^2 + (x_3 - 0.02)^2} - p_0,$$

$$\phi_1(x_1, x_2, x_3) = 0.5 + 0.5 \cos(x_1 x_2 x_3), \quad \text{and} \quad \phi_2(x_1, x_2, x_3) = 0.1 + 0.3 \exp(x_1 x_2 x_3).$$

Tables 5.7 and 5.8 along with Figure 5.4 confirm a disturbed convergence under quasi-uniform refinement, whereas optimal convergence rates are obtained when adaptive refinements guided by the *a posteriori* error estimator Θ , with $k = 0$, are used. In turn, the initial mesh and some approximated solutions after four mesh refinement steps (via Θ) are collected in Figure 5.5. In particular, we see there that the pressure presents high values and hence, most likely, high gradients as well near the contraction region of the 3D L-shape domain, as we expected. The latter is complemented with Figure 5.6, where snapshots of three meshes via Θ show a clustering of elements in the same region.

Example 4: Flow through a 2D porous media with channel network.

Inspired by [5, Example 3, Section 6], we finally focus on a flow through a porous medium with a channel network considering strong jump discontinuities of the parameters \mathbf{F} and \mathbf{K} across the two regions. We consider the square domain $\Omega = (-1, 1)^2$ with an internal channel network denoted as Ω_c (see the first plot of Figure 5.7 below), and boundary Γ , whose left, right, upper and lower parts are given by $\Gamma_{\text{left}} = \{-1\} \times (-1, 1)$, $\Gamma_{\text{right}} = \{1\} \times (-1, 1)$, $\Gamma_{\text{top}} = (-1, 1) \times \{1\}$, and $\Gamma_{\text{bottom}} = (-1, 1) \times \{-1\}$, respectively. We consider the coupling of the Brinkman–Forchheimer and double-diffusion equations (2.7) in the whole domain Ω with $\mathbf{Q}_1 = 0.5 \mathbb{I}$ and $\mathbf{Q}_2 = 0.125 \mathbb{I}$, but with different values of the parameters \mathbf{F} and $\mathbf{K} = \alpha \mathbb{I}$ for the interior and the exterior of the channel, namely

$$\mathbf{F} = \begin{cases} 10 & \text{in } \Omega_c \\ 1 & \text{in } \overline{\Omega} \setminus \Omega_c \end{cases} \quad \text{and} \quad \alpha = \begin{cases} 1 & \text{in } \Omega_c \\ 0.001 & \text{in } \overline{\Omega} \setminus \Omega_c \end{cases}.$$

The parameter choice corresponds to increased inertial effect ($\mathbf{F} = 10$) in the channel and a high permeability ($\alpha = 1$), compared to reduced inertial effect ($\mathbf{F} = 1$) in the porous medium and low permeability ($\alpha = 0.001$). In addition, the boundary conditions are

$$\begin{aligned} \mathbf{u} \cdot \mathbf{n} &= 0.2, \quad \mathbf{u} \cdot \boldsymbol{\tau} = 0 \quad \text{on } \Gamma_{\text{left}}, \quad \boldsymbol{\sigma} \mathbf{n} = \mathbf{0} \quad \text{on } \Gamma \setminus \Gamma_{\text{left}}, \\ \phi_1 &= 0.3 \quad \text{on } \Gamma_{\text{bottom}}, \quad \phi_1 = 0 \quad \text{on } \Gamma_{\text{top}}, \quad \boldsymbol{\rho}_1 \cdot \mathbf{n} = 0 \quad \text{on } \Gamma_{\text{left}} \cup \Gamma_{\text{right}}, \\ \phi_2 &= 0.2 \quad \text{on } \Gamma_{\text{bottom}}, \quad \phi_2 = 0 \quad \text{on } \Gamma_{\text{top}}, \quad \boldsymbol{\rho}_2 \cdot \mathbf{n} = 0 \quad \text{on } \Gamma_{\text{left}} \cup \Gamma_{\text{right}}. \end{aligned}$$

In particular, the first row of boundary equations corresponds to inflow on the left boundary and zero stress outflow on the rest of the boundary. In Figure 5.7, for the sake of simplicity, we only display the computed magnitude of the velocity and velocity gradient tensor, which were built using

the $\mathbf{P}_0 - \mathbb{P}_0 - \mathbb{RT}_0 - \mathbf{P}_0 - \mathbf{P}_0 - \mathbf{RT}_0$ scheme on a mesh with 48,429 triangle elements (actually representing 824,663 DOF) obtained via Θ . Similarly to [5, Example 3, Section 6], faster flow through the channel network, with a significant velocity gradient across the interface between the porous medium and the channel, are observed. These results are in agreement with those obtained in [5] but now taking into account that the mesh employed was obtained through an adaptive refinement process guided by the *a posteriori* error indicator Θ . In turn, snapshots of some adapted meshes generated using Θ are depicted in Figure 5.8. We can observe a suitable refinement around the interface that couples the porous medium with the channel network as well as the region near the inflow boundary. The latter suggest that the indicator Θ is able to detect the strong jump discontinuities of the model parameters along the interface between the channel and porous media, as we expected.

DOF	iter	$e(\mathbf{u})$	$r(\mathbf{u})$	$e(\mathbf{t})$	$r(\mathbf{t})$	$e(\boldsymbol{\sigma})$	$r(\boldsymbol{\sigma})$	$e(p)$	$r(p)$
644	5	8.09E-01	–	7.68E+00	–	6.68E+01	–	3.60E+00	–
2818	5	4.05E-01	0.94	3.97E+00	0.89	3.52E+01	0.87	1.44E+00	1.24
10464	5	2.22E-01	0.92	2.12E+00	0.96	1.86E+01	0.97	7.50E-01	0.99
41124	5	1.11E-01	1.01	1.08E+00	0.98	9.33E+00	1.01	3.72E-01	1.02
164698	5	5.58E-02	1.00	5.43E-01	0.99	4.67E+00	1.00	1.85E-01	1.01
665758	5	2.78E-02	1.00	2.69E-01	1.01	2.32E+00	1.00	9.14E-02	1.01

$e(\phi)$	$r(\phi)$	$e(\tilde{\mathbf{t}})$	$r(\tilde{\mathbf{t}})$	$e(\boldsymbol{\rho})$	$r(\boldsymbol{\rho})$	$e(\vec{\boldsymbol{\sigma}})$	$r(\vec{\boldsymbol{\sigma}})$	Θ	eff(Θ)
3.52E+00	–	1.14E+01	–	3.26E+01	–	1.23E+02	–	1.52E+02	0.806
1.85E+00	0.87	5.76E+00	0.93	1.55E+01	1.01	6.27E+01	0.91	8.50E+01	0.738
9.19E-01	1.07	2.97E+00	1.01	7.86E+00	1.03	3.27E+01	0.99	4.50E+01	0.727
4.41E-01	1.08	1.50E+00	1.00	3.96E+00	1.00	1.64E+01	1.01	2.29E+01	0.718
2.24E-01	0.97	7.48E-01	1.00	1.98E+00	1.00	8.23E+00	1.00	1.15E+01	0.718
1.10E-01	1.02	3.72E-01	1.00	9.82E-01	1.01	4.08E+00	1.00	5.70E+00	0.716

Table 5.1: [EXAMPLE 1] $\mathbf{P}_0 - \mathbb{P}_0 - \mathbb{RT}_0 - \mathbf{P}_0 - \mathbf{P}_0 - \mathbf{RT}_0$ scheme with quasi-uniform refinement.

DOF	iter	$e(\mathbf{u})$	$r(\mathbf{u})$	$e(\mathbf{t})$	$r(\mathbf{t})$	$e(\boldsymbol{\sigma})$	$r(\boldsymbol{\sigma})$	$e(p)$	$r(p)$
1972	5	3.83E-01	–	4.01E+00	–	3.07E+01	–	1.08E+00	–
8714	5	9.17E-02	1.93	8.86E-01	2.03	8.41E+00	1.74	2.75E-01	1.84
32480	5	2.49E-02	1.98	2.41E-01	1.98	2.35E+00	1.94	7.20E-02	2.04
127924	5	6.34E-03	1.99	5.97E-02	2.04	5.99E-01	1.99	1.71E-02	2.10
512898	5	1.59E-03	1.99	1.52E-02	1.97	1.50E-01	1.99	4.33E-03	1.97
2074454	5	3.86E-04	2.02	3.74E-03	2.00	3.66E-02	2.02	1.06E-03	2.02

$e(\phi)$	$r(\phi)$	$e(\tilde{\mathbf{t}})$	$r(\tilde{\mathbf{t}})$	$e(\boldsymbol{\rho})$	$r(\boldsymbol{\rho})$	$e(\vec{\boldsymbol{\sigma}})$	$r(\vec{\boldsymbol{\sigma}})$	Θ	eff(Θ)
5.64E-01	–	2.20E+00	–	8.71E+00	–	4.66E+01	–	7.54E+01	0.617
1.36E-01	1.91	5.48E-01	1.87	1.95E+00	2.01	1.20E+01	1.82	2.00E+01	0.600
3.87E-02	1.91	1.45E-01	2.02	5.13E-01	2.03	3.31E+00	1.96	5.52E+00	0.599
1.04E-02	1.91	3.76E-02	1.97	1.30E-01	2.00	8.44E-01	1.99	1.41E+00	0.598
2.35E-03	2.15	9.37E-03	2.00	3.27E-02	1.99	2.12E-01	1.99	3.53E-01	0.599
5.88E-04	1.98	2.28E-03	2.02	7.97E-03	2.02	5.16E-02	2.02	8.63E-02	0.598

Table 5.2: [EXAMPLE 1] $\mathbf{P}_1 - \mathbb{P}_1 - \mathbb{RT}_1 - \mathbf{P}_1 - \mathbf{P}_1 - \mathbf{RT}_1$ scheme with quasi-uniform refinement.

DOF	iter	$e(\mathbf{u})$	$r(\mathbf{u})$	$e(\mathbf{t})$	$r(\mathbf{t})$	$e(\boldsymbol{\sigma})$	$r(\boldsymbol{\sigma})$	$e(p)$	$r(p)$
1832	8	1.35E+01	–	1.81E+02	–	8.63E+03	–	3.44E+02	–
7608	7	1.35E+01	–	2.51E+02	–	1.14E+04	–	3.56E+02	–
29666	6	1.03E+01	0.40	2.79E+02	–	1.06E+04	0.11	2.76E+02	0.37
117710	6	5.09E+00	1.02	2.20E+02	0.35	7.65E+03	0.48	1.86E+02	0.57
470938	6	1.91E+00	1.41	1.39E+02	0.66	4.64E+03	0.72	1.03E+02	0.85
1887552	6	5.24E-01	1.86	7.20E+01	0.94	2.44E+03	0.92	5.15E+01	1.00

$e(\phi)$	$r(\phi)$	$e(\tilde{\mathbf{t}})$	$r(\tilde{\mathbf{t}})$	$e(\boldsymbol{\rho})$	$r(\boldsymbol{\rho})$	$e(\tilde{\boldsymbol{\sigma}})$	$r(\tilde{\boldsymbol{\sigma}})$	Θ	eff(Θ)
2.26E+01	–	1.44E+02	–	1.62E+03	–	1.06E+04	–	1.05E+04	1.008
1.18E+01	0.91	9.89E+01	0.53	1.20E+03	0.42	1.30E+04	–	1.31E+04	0.995
6.25E+00	0.94	5.90E+01	0.76	7.37E+02	0.72	1.17E+04	0.15	1.19E+04	0.986
3.11E+00	1.01	3.08E+01	0.94	3.81E+02	0.96	8.29E+03	0.50	8.44E+03	0.982
1.64E+00	0.93	1.59E+01	0.95	1.95E+02	0.97	4.99E+03	0.73	5.14E+03	0.971
8.25E-01	0.99	7.97E+00	1.00	9.74E+01	1.00	2.62E+03	0.93	2.69E+03	0.973

Table 5.3: [EXAMPLE 2] $\mathbf{P}_0 - \mathbb{P}_0 - \mathbb{RT}_0 - \mathbf{P}_0 - \mathbf{P}_0 - \mathbf{RT}_0$ scheme with quasi-uniform refinement.

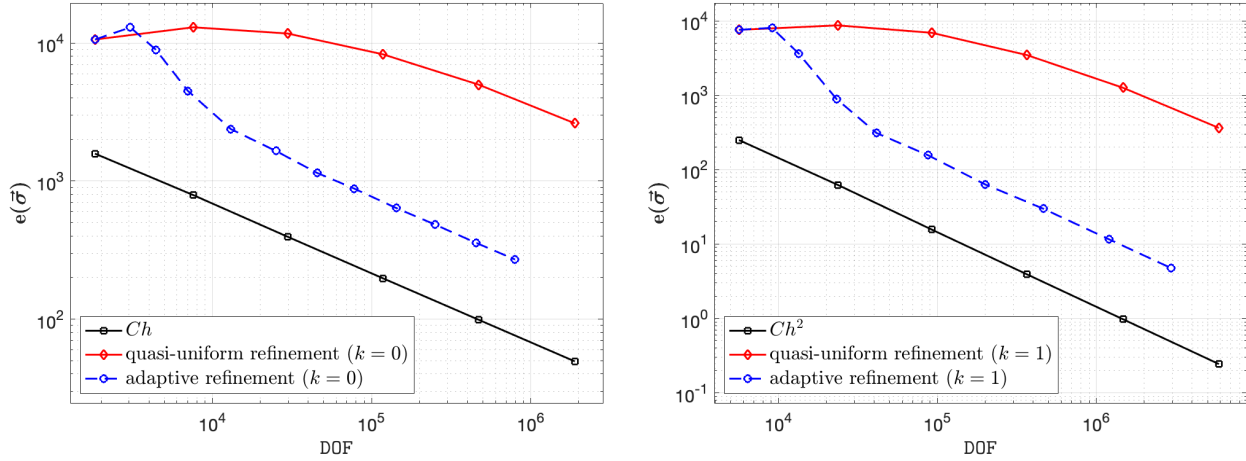


Figure 5.1: [EXAMPLE 2] Log-log plots of $e(\boldsymbol{\sigma})$ vs. DOF for quasi-uniform/adaptative schemes via Θ for $k = 0$ and $k = 1$ (left and right plots, respectively).

References

- [1] S. AGMON, *Lectures on Elliptic Boundary Value Problems*. Van Nostrand, Princeton, NJ, 1965.
- [2] T.P. BARRIOS, G.N. GATICA, M. GONZÁLEZ, AND N. HEUER, *A residual based a posteriori error estimator for an augmented mixed finite element method in linear elasticity*. M2AN Math. Model. Numer. Anal. 40 (2006), no. 5, 843–869.
- [3] J. CAMAÑO, S. CAUCAO, R. OYARZÚA, AND S. VILLA-FUENTES, *A posteriori error analysis of a momentum conservative Banach spaces based mixed-FEM for the Navier–Stokes problem*. Appl. Numer. Math. 176 (2022), 134–158.

DOF	iter	$e(\mathbf{u})$	$r(\mathbf{u})$	$e(\mathbf{t})$	$r(\mathbf{t})$	$e(\boldsymbol{\sigma})$	$r(\boldsymbol{\sigma})$	$e(p)$	$r(p)$
5640	7	9.83E+00	–	2.16E+02	–	6.50E+03	–	2.22E+02	–
23576	6	6.97E+00	0.48	2.23E+02	–	7.95E+03	–	1.96E+02	0.18
92202	6	2.75E+00	1.36	1.38E+02	0.70	6.54E+03	0.29	1.13E+02	0.81
366406	6	8.26E-01	1.74	7.01E+01	0.98	3.32E+03	0.98	5.38E+01	1.07
1467074	6	1.78E-01	2.21	2.52E+01	1.47	1.22E+03	1.45	1.74E+01	1.62
5882432	6	2.42E-02	2.87	6.83E+00	1.88	3.52E+02	1.79	4.90E+00	1.83

$e(\phi)$	$r(\phi)$	$e(\tilde{\mathbf{t}})$	$r(\tilde{\mathbf{t}})$	$e(\boldsymbol{\rho})$	$r(\boldsymbol{\rho})$	$e(\tilde{\boldsymbol{\sigma}})$	$r(\tilde{\boldsymbol{\sigma}})$	Θ	eff(Θ)
6.94E+00	–	5.91E+01	–	7.75E+02	–	7.57E+03	–	8.13E+03	0.931
2.79E+00	1.28	2.93E+01	0.98	4.80E+02	0.67	8.70E+03	–	9.19E+03	0.946
1.03E+00	1.46	1.17E+01	1.34	2.11E+02	1.20	6.91E+03	0.34	7.46E+03	0.926
2.68E-01	1.95	3.47E+00	1.76	6.40E+01	1.73	3.46E+03	1.00	3.77E+03	0.917
7.96E-02	1.75	9.89E-01	1.81	1.80E+01	1.83	1.26E+03	1.46	1.38E+03	0.915
2.09E-02	1.93	2.52E-01	1.97	4.60E+00	1.97	3.64E+02	1.79	3.95E+02	0.921

Table 5.4: [EXAMPLE 2] $\mathbf{P}_1 - \mathbb{P}_1 - \mathbb{RT}_1 - \mathbf{P}_1 - \mathbf{P}_1 - \mathbf{RT}_1$ scheme with quasi-uniform refinement.

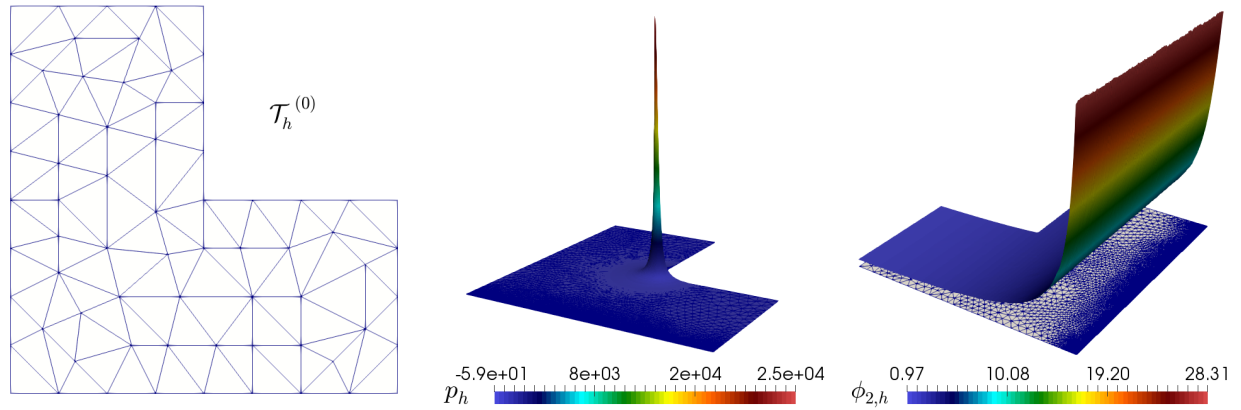


Figure 5.2: [EXAMPLE 2] Initial mesh, computed pressure and concentration fields.

- [4] S. CAUCAO, M. DISCACCIATI, G.N. GATICA, AND R. OYARZÚA, *A conforming mixed finite element method for the Navier–Stokes/Darcy–Forchheimer coupled problem*. ESAIM Math. Model. Numer. Anal. 54 (2020), no. 5, 1689–1723.
- [5] S. CAUCAO, G.N. GATICA, AND J.P. ORTEGA, *A fully-mixed formulation in Banach spaces for the coupling of the steady Brinkman–Forchheimer and double-diffusion equations*. ESAIM Math. Model. Numer. Anal. 55 (2021), no. 6, 2725–2758.
- [6] S. CAUCAO, G.N. GATICA, AND R. OYARZÚA, *A posteriori error analysis of a fully-mixed formulation for the Navier–Stokes/Darcy coupled problem with nonlinear viscosity*. Comput. Methods Appl. Mech. Engrg. 315 (2017), 943–971.
- [7] S. CAUCAO, G.N. GATICA, AND R. OYARZÚA, *A posteriori error analysis of an augmented fully mixed formulation for the nonisothermal Oldroyd–Stokes problem*. Numer. Methods Partial Differential Equations 35 (2019), no. 1, 295–324.

DOF	iter	$e(\mathbf{u})$	$r(\mathbf{u})$	$e(\mathbf{t})$	$r(\mathbf{t})$	$e(\boldsymbol{\sigma})$	$r(\boldsymbol{\sigma})$	$e(p)$	$r(p)$
1832	8	1.35E+01	–	1.81E+02	–	8.63E+03	–	3.44E+02	–
3057	6	1.09E+01	0.84	2.54E+02	–	1.12E+04	–	2.98E+02	0.56
4422	6	3.81E+00	5.70	1.90E+02	1.57	7.29E+03	2.31	1.59E+02	3.42
7023	6	1.13E+00	5.25	8.77E+01	3.34	3.21E+03	3.54	6.87E+01	3.62
13072	6	1.01E+00	0.36	4.84E+01	1.91	1.52E+03	2.41	3.78E+01	1.92
25059	6	8.71E-01	0.46	3.42E+01	1.07	9.97E+02	1.30	2.64E+01	1.11
45447	6	7.85E-01	0.35	2.52E+01	1.02	7.46E+02	0.97	1.94E+01	1.04
77578	6	5.98E-01	1.02	1.90E+01	1.05	5.66E+02	1.03	1.42E+01	1.15
142989	6	4.51E-01	0.92	1.44E+01	0.92	4.26E+02	0.93	1.06E+01	0.96
250193	6	3.15E-01	1.28	1.09E+01	0.98	3.24E+02	0.98	8.02E+00	1.00
452423	6	2.42E-01	0.89	8.33E+00	0.91	2.49E+02	0.89	6.10E+00	0.93
795326	6	1.74E-01	1.18	6.33E+00	0.97	1.89E+02	0.97	4.63E+00	0.98

$e(\phi)$	$r(\phi)$	$e(\tilde{\mathbf{t}})$	$r(\tilde{\mathbf{t}})$	$e(\boldsymbol{\rho})$	$r(\boldsymbol{\rho})$	$e(\vec{\boldsymbol{\sigma}})$	$r(\vec{\boldsymbol{\sigma}})$	Θ	eff(Θ)
2.26E+01	–	1.44E+02	–	1.62E+03	–	1.06E+04	–	1.05E+04	1.008
1.71E+01	1.10	1.33E+02	0.32	1.41E+03	0.56	1.30E+04	–	1.29E+04	1.006
1.49E+01	0.75	1.19E+02	0.61	1.32E+03	0.33	8.94E+03	2.02	8.80E+03	1.015
9.87E+00	1.78	9.21E+01	1.09	1.09E+03	0.82	4.50E+03	2.97	4.40E+03	1.022
6.05E+00	1.58	5.81E+01	1.48	7.44E+02	1.24	2.38E+03	2.05	2.33E+03	1.020
4.26E+00	1.08	4.38E+01	0.86	5.73E+02	0.81	1.65E+03	1.12	1.62E+03	1.021
2.52E+00	1.76	2.58E+01	1.78	3.46E+02	1.69	1.15E+03	1.23	1.13E+03	1.014
1.91E+00	1.05	2.05E+01	0.86	2.75E+02	0.86	8.83E+02	0.97	8.71E+02	1.014
1.29E+00	1.29	1.35E+01	1.37	1.82E+02	1.35	6.37E+02	1.07	6.31E+02	1.010
9.61E-01	1.04	1.02E+01	0.99	1.38E+02	0.99	4.84E+02	0.98	4.79E+02	1.010
6.50E-01	1.32	6.82E+00	1.37	9.19E+01	1.37	3.57E+02	1.03	3.55E+02	1.006
4.83E-01	1.05	5.11E+00	1.03	6.90E+01	1.02	2.70E+02	0.99	2.69E+02	1.006

Table 5.5: [EXAMPLE 2] $\mathbf{P}_0 - \mathbb{P}_0 - \mathbb{RT}_0 - \mathbf{P}_0 - \mathbf{P}_0 - \mathbf{RT}_0$ scheme with adaptive refinement via Θ .

- [8] S. CAUCAO, G.N. GATICA, R. OYARZÚA, AND N. SÁNCHEZ, *A fully-mixed formulation for the steady double-diffusive convection system based upon Brinkman–Forchheimer equations*. J. Sci. Comput. 85 (2020), no. 2, Paper No. 44, 37 pp.
- [9] S. CAUCAO, G.N. GATICA, R. OYARZÚA, AND F. SANDOVAL, *Residual-based a posteriori error analysis for the coupling of the Navier–Stokes and Darcy–Forchheimer equations*. ESAIM: Math. Model. Numer. Anal. 55 (2021), no. 2, 659–687.
- [10] S. CAUCAO, G.N. GATICA, R. OYARZÚA, AND P. ZÚÑIGA, *A posteriori error analysis of a mixed finite element method for the coupled Brinkman–Forchheimer and double-diffusion equations*. Preprint 2022-11, Centro de Investigación en Ingeniería Matemática (CI²MA), Universidad de Concepción, Chile, (2022).
- [11] P. CLÉMENT, *Approximation by finite element functions using local regularisation*. RAIRO Modélisation Mathématique et Analyse Numérique 9 (1975), 77–84.
- [12] E. COLMENARES, G.N. GATICA, AND S. MORAGA, *A Banach spaces-based analysis of a new fully-mixed finite element method for the Boussinesq problem*. ESAIM Math. Model. Numer. Anal. 54 (2020), no. 5, 1525–1568.

Dof	iter	$e(\mathbf{u})$	$r(\mathbf{u})$	$e(\mathbf{t})$	$r(\mathbf{t})$	$e(\boldsymbol{\sigma})$	$r(\boldsymbol{\sigma})$	$e(p)$	$r(p)$
5640	7	9.83E+00	–	2.16E+02	–	6.50E+03	–	2.22E+02	–
9105	6	4.34E+00	3.41	1.72E+02	0.96	7.14E+03	–	1.32E+02	2.16
13393	6	5.77E-01	10.45	5.41E+01	5.98	2.90E+03	4.66	4.49E+01	5.61
23159	6	1.05E-01	6.21	1.09E+01	5.86	5.62E+02	6.00	7.99E+00	6.30
41452	6	1.01E-01	0.15	4.78E+00	2.81	1.67E+02	4.17	3.51E+00	2.83
87093	6	8.66E-02	0.41	1.87E+00	2.53	7.49E+01	2.16	1.34E+00	2.59
198988	6	5.82E-02	0.96	1.13E+00	1.21	3.85E+01	1.61	8.13E-01	1.21
462786	6	1.67E-02	2.96	4.00E-01	2.47	1.64E+01	2.02	2.87E-01	2.47
1195614	6	8.38E-03	1.45	2.11E-01	1.35	7.38E+00	1.68	1.53E-01	1.33
2935459	6	2.34E-03	2.84	6.81E-02	2.52	2.70E+00	2.24	4.91E-02	2.53

$e(\phi)$	$r(\phi)$	$e(\tilde{\mathbf{t}})$	$r(\tilde{\mathbf{t}})$	$e(\boldsymbol{\rho})$	$r(\boldsymbol{\rho})$	$e(\tilde{\boldsymbol{\sigma}})$	$r(\tilde{\boldsymbol{\sigma}})$	Θ	eff(Θ)
6.94E+00	–	5.91E+01	–	7.75E+02	–	7.57E+03	–	8.13E+03	0.931
5.96E+00	0.64	4.98E+01	0.71	6.91E+02	0.48	8.06E+03	–	8.40E+03	0.960
4.60E+00	1.33	4.46E+01	0.57	6.33E+02	0.46	3.64E+03	4.12	3.76E+03	0.969
1.49E+00	4.13	1.68E+01	3.56	3.02E+02	2.71	8.93E+02	5.13	9.13E+02	0.978
6.00E-01	3.11	6.88E+00	3.07	1.31E+02	2.87	3.10E+02	3.63	3.20E+02	0.968
3.02E-01	1.85	3.88E+00	1.54	7.54E+01	1.48	1.56E+02	1.84	1.61E+02	0.972
9.88E-02	2.70	1.17E+00	2.91	2.26E+01	2.92	6.35E+01	2.18	6.65E+01	0.955
4.49E-02	1.87	6.17E-01	1.51	1.24E+01	1.42	2.99E+01	1.79	3.07E+01	0.974
1.59E-02	2.19	1.96E-01	2.42	3.82E+00	2.48	1.16E+01	1.99	1.21E+01	0.958
6.72E-03	1.91	9.50E-02	1.61	1.91E+00	1.55	4.77E+00	1.98	4.90E+00	0.975

Table 5.6: [EXAMPLE 2] $\mathbf{P}_1 - \mathbb{P}_1 - \mathbb{RT}_1 - \mathbf{P}_1 - \mathbf{P}_1 - \mathbf{RT}_1$ scheme with adaptive refinement via Θ .

- [13] E. COLMENARES, G.N. GATICA, S. MORAGA, AND R. RUIZ-BAIER, *A fully-mixed finite element method for the steady state Oberbeck-Boussinesq system*. SMAI J. Comput. Math. 6 (2020), 125–157.
- [14] E. COLMENARES, G.N. GATICA, AND R. OYARZÚA, *A posteriori error analysis of an augmented mixed-primal formulation for the stationary Boussinesq model*. Calcolo 54 (2017), no. 3, 1055–1095.
- [15] E. COLMENARES, G.N. GATICA, AND R. OYARZÚA, *A posteriori error analysis of an augmented fully-mixed formulation for the stationary Boussinesq model*. Comput. Math. Appl. 77 (2019), no. 3, 693–714.
- [16] E. CREUSE, M. FARHLOUL, AND L. PAQUET, *A posteriori error estimation for the dual mixed finite element method for the p -Laplacian in a polygonal domain*. Comput. Methods Appl. Mech. Engrg. 196 (2007), no. 25–28, 2570–2582.
- [17] A. ERN AND J.-L. GUERMOND, *Theory and Practice of Finite Elements*. Applied Mathematical Sciences, 159. Springer-Verlag, New York, 2004.
- [18] V.J. ERVIN AND T.N. PHILLIPS, *Residual a posteriori error estimator for a three-field model of a non-linear generalized Stokes problem*. Comput. Methods Appl. Mech. Engrg. 195 (2006), no. 19–22, 2599–2610.

DOF	iter	e(u)	r(u)	e(t)	r(t)	e(σ)	r(σ)	e(p)	r(p)
4456	5	5.14E-01	–	5.94E+00	–	1.58E+02	–	9.39E+00	–
67000	4	2.96E-01	0.61	5.42E+00	0.10	1.50E+02	0.06	7.53E+00	0.24
271744	4	1.97E-01	0.87	4.79E+00	0.26	1.37E+02	0.19	5.90E+00	0.52
703252	4	1.35E-01	1.19	4.11E+00	0.48	1.18E+02	0.47	4.60E+00	0.79
1446088	4	9.80E-02	1.34	3.57E+00	0.58	1.02E+02	0.62	3.72E+00	0.88

e(ϕ)	r(ϕ)	e(\tilde{t})	r(\tilde{t})	e(ρ)	r(ρ)	e($\vec{\sigma}$)	r($\vec{\sigma}$)	Θ	eff(Θ)
2.06E-02	–	1.29E-01	–	2.47E-01	–	1.64E+02	–	1.50E+02	1.099
1.20E-02	0.59	6.45E-02	0.76	1.19E-01	0.81	1.56E+02	0.06	1.41E+02	1.107
7.34E-03	1.06	4.03E-02	1.01	7.45E-02	1.00	1.42E+02	0.20	1.29E+02	1.099
4.71E-03	1.39	2.78E-02	1.18	5.03E-02	1.24	1.22E+02	0.47	1.12E+02	1.095
3.22E-03	1.59	2.05E-02	1.27	3.65E-02	1.33	1.05E+02	0.62	9.63E+01	1.093

Table 5.7: [EXAMPLE 3] $\mathbf{P}_0 - \mathbb{P}_0 - \mathbb{RT}_0 - \mathbf{P}_0 - \mathbf{P}_0 - \mathbf{RT}_0$ scheme with quasi-uniform refinement.

DOF	iter	e(u)	r(u)	e(t)	r(t)	e(σ)	r(σ)	e(p)	r(p)
4456	5	5.14E-01	–	5.94E+00	–	1.58E+02	–	9.39E+00	–
10246	5	5.54E-01	–	6.23E+00	–	1.65E+02	–	1.12E+01	–
52750	4	2.91E-01	1.18	5.41E+00	0.26	1.56E+02	0.10	6.90E+00	0.89
144226	4	1.41E-01	2.16	4.02E+00	0.88	1.14E+02	0.93	4.22E+00	1.46
915951	4	6.09E-02	1.37	2.34E+00	0.88	6.23E+01	0.98	2.02E+00	1.20

e(ϕ)	r(ϕ)	e(\tilde{t})	r(\tilde{t})	e(ρ)	r(ρ)	e($\vec{\sigma}$)	r($\vec{\sigma}$)	Θ	eff(Θ)
2.06E-02	–	1.29E-01	–	2.47E-01	–	1.64E+02	–	1.50E+02	1.099
2.49E-02	–	1.41E-01	–	2.35E-01	0.17	1.72E+02	–	1.53E+02	1.126
1.07E-02	1.55	6.44E-02	1.44	1.17E-01	1.28	1.62E+02	0.11	1.47E+02	1.098
5.27E-03	2.11	3.90E-02	1.49	7.02E-02	1.52	1.18E+02	0.94	1.08E+02	1.091
2.48E-03	1.22	2.00E-02	1.09	3.72E-02	1.03	6.47E+01	0.98	5.94E+01	1.090

Table 5.8: [EXAMPLE 3] $\mathbf{P}_0 - \mathbb{P}_0 - \mathbb{RT}_0 - \mathbf{P}_0 - \mathbf{P}_0 - \mathbf{RT}_0$ scheme with adaptive refinement via Θ .

- [19] M. FARHLOUL AND A.M. ZINE, *A posteriori error estimation for a dual mixed finite element approximation of non-Newtonian fluid flow problems*. Int. J. Numer. Anal. Model. 5 (2008), no. 2, 320–330.
- [20] G.N. GATICA, *A note on stable Helmholtz decompositions in 3D*. Appl. Anal. 99 (2020), no. 7, 1110–1121.
- [21] G.N. GATICA, *A Simple Introduction to the Mixed Finite Element Method. Theory and Applications*. SpringerBriefs in Mathematics. Springer, Cham, 2014.
- [22] G.N. GATICA, L.F. GATICA, AND F. SEQUEIRA, *A priori and a posteriori error analyses of a pseudostress-based mixed formulation for linear elasticity*. Comput. Math. Appl. 71 (2016), no. 2, 585–614.

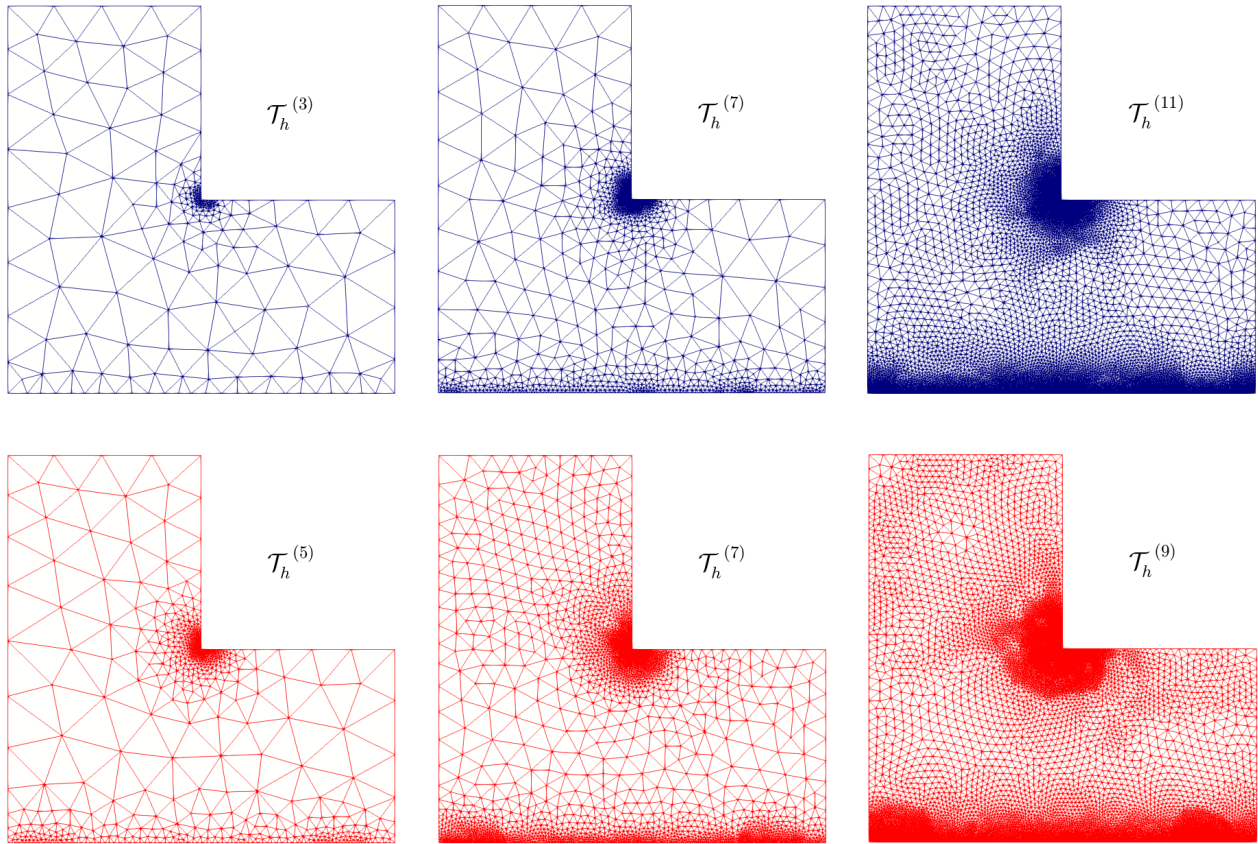


Figure 5.3: [EXAMPLE 2] Three snapshots of adapted meshes according to the indicator Θ for $k = 0$ and $k = 1$ (top and bottom plots, respectively).

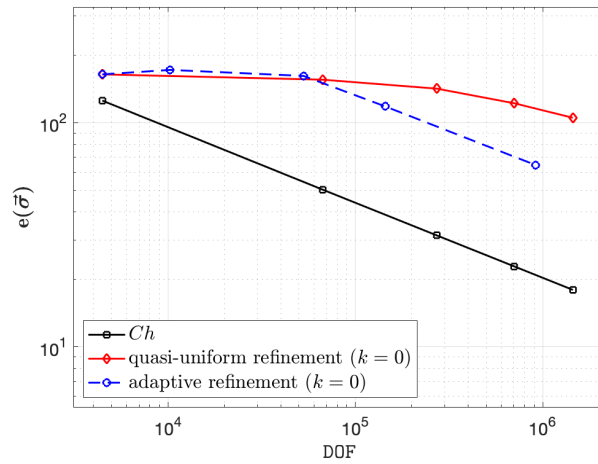


Figure 5.4: [EXAMPLE 3] Log-log plot of $e(\vec{\sigma})$ vs. DOF for quasi-uniform/adaptative schemes via Θ for $k = 0$.

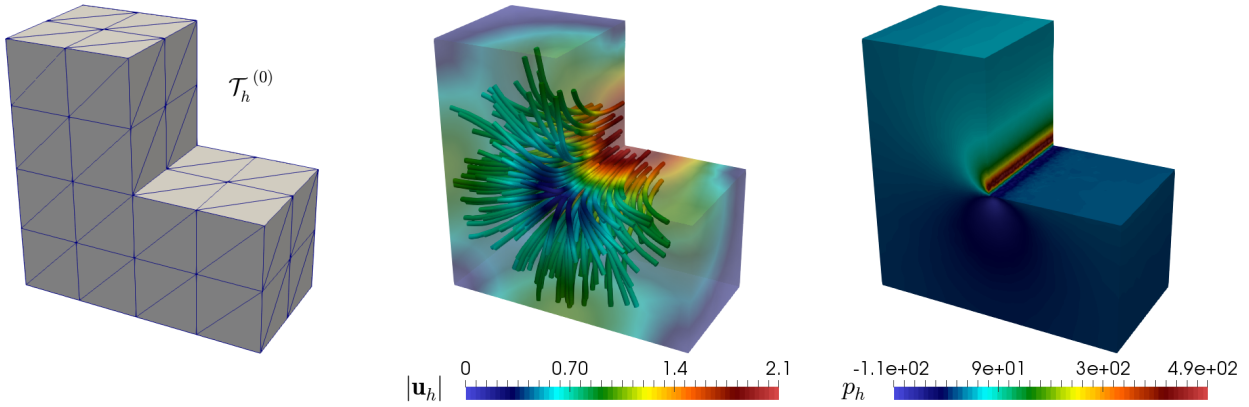


Figure 5.5: [EXAMPLE 3] Initial mesh, computed magnitude of the velocity, and pressure field.

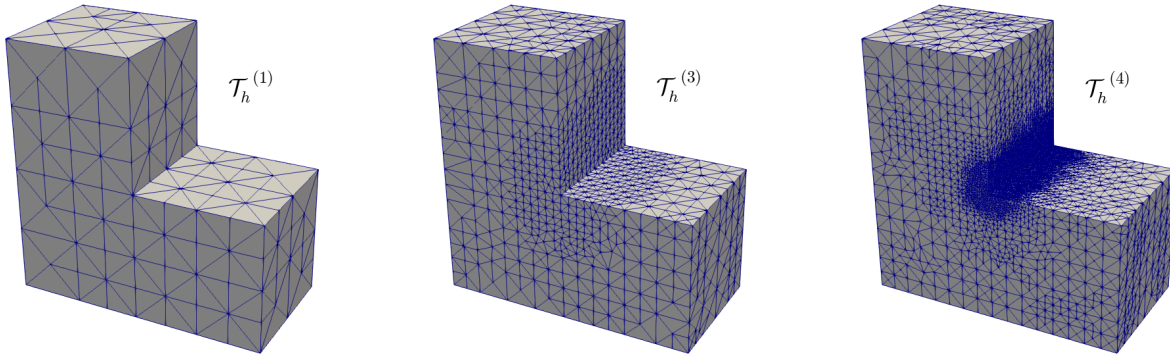


Figure 5.6: [EXAMPLE 3] Three snapshots of adapted meshes according to the indicator Θ for $k = 0$.

- [23] G.N. GATICA, C. INZUNZA, R. RUIZ-BAIER, AND F. SANDOVAL, *A posteriori error analysis of Banach spaces-based fully-mixed finite element methods for Boussinesq-type models*. J. Numer. Math., to appear.
- [24] G.N. GATICA, A. MÁRQUEZ, AND M.A. SÁNCHEZ, *Analysis of a velocity-pressure-pseudostress formulation for the stationary Stokes equations*. Comput. Methods Appl. Mech. Engrg. 199 (2010), 1064–1079.
- [25] G.N. GATICA, R. RUIZ-BAIER, AND G. TIERRA, *A posteriori error analysis of an augmented mixed method for the Navier–Stokes equations with nonlinear viscosity*. Comput. Math. Appl. 72 (2016), no. 9, 2289–2310.
- [26] V. GIRAULT AND P.A. RAVIART, *Finite Element Methods for Navier–Stokes Equations. Theory and Algorithms*. Springer Series in Computational Mathematics, 5. Springer-Verlag, Berlin, 1986.
- [27] F. HECHT, *New development in FreeFem++*. J. Numer. Math. 20 (2012), 251–265.
- [28] F. HECHT, *FreeFem++*. Third Edition, Version 3.58-1. Laboratoire Jacques-Louis Lions, Université Pierre et Marie Curie, Paris, 2018. [available in <http://www.freefem.org/ff++>].

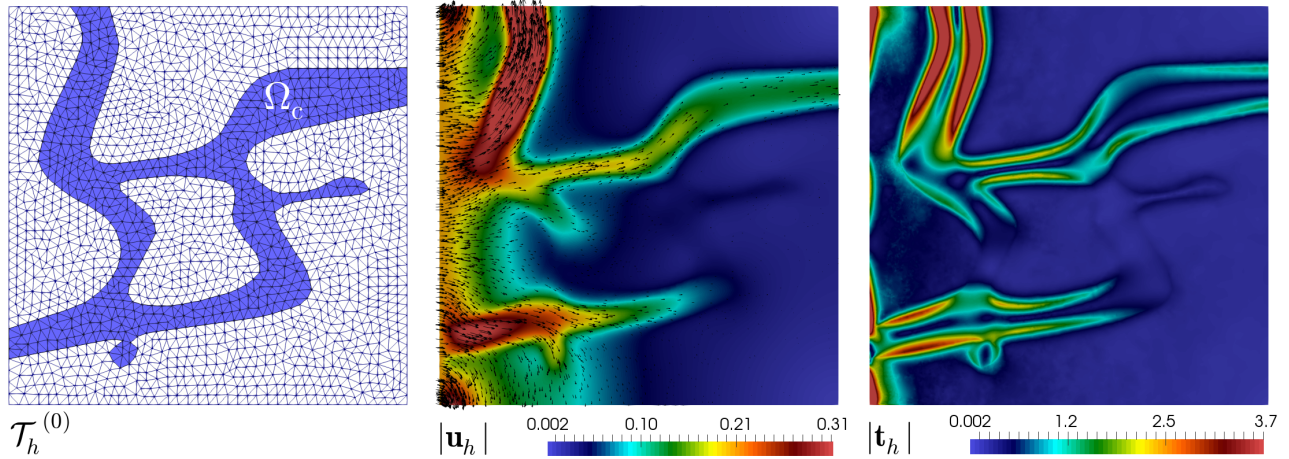


Figure 5.7: [EXAMPLE 4] Initial mesh, computed magnitude of the velocity, and velocity gradient tensor.

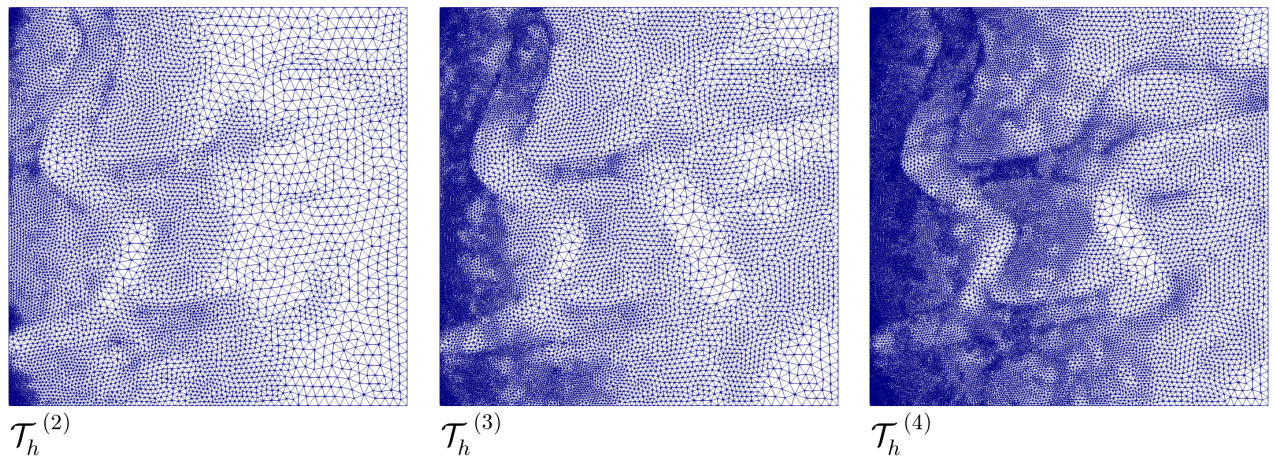


Figure 5.8: [EXAMPLE 4] Three snapshots of adapted meshes according to the indicator Θ for $k = 0$.

- [29] P.N. KALONI AND J. GUO, *Steady nonlinear double-diffusive convection in a porous medium based upon the Brinkman–Forchheimer model*. J. Math. Anal. Appl. 204 (1996), no. 1, 138–155.
- [30] T. SAYAH, *A posteriori error estimates for the Brinkman–Darcy–Forchheimer problem*. Comput. Appl. Math. 40 (2021), no. 7, Paper No. 256, 38 pp.
- [31] R. VERFÜRTH, *A Review of A-Posteriori Error Estimation and Adaptive Mesh-Refinement Techniques*. Wiley Teubner, Chichester, 1996.

Centro de Investigación en Ingeniería Matemática (CI²MA)

PRE-PUBLICACIONES 2022

- 2022-01 NESTOR SÁNCHEZ, TONATIUH SANCHEZ-VIZUET, MANUEL SOLANO: *Afternote to Coupling at a distance: convergence analysis and a priori error estimates*
- 2022-02 GABRIEL N. GATICA, CRISTIAN INZUNZA, FILANDER A. SEQUEIRA: *A pseudostress-based mixed-primal finite element method for stress-assisted diffusion problems in Banach spaces*
- 2022-03 ELIGIO COLMENARES, RICARDO OYARZÚA, FRANCISCO PIÑA: *A fully-DG method for the stationary Boussinesq system*
- 2022-04 JUAN MANUEL CÁRDENAS, MANUEL SOLANO: *A high order unfitted hybridizable discontinuous Galerkin method for linear elasticity*
- 2022-05 JAIME MANRÍQUEZ, NGOC-CUONG NGUYEN, MANUEL SOLANO: *A dissimilar non-matching HDG discretization for Stokes flows*
- 2022-06 RAIMUND BÜRGER, STEFAN DIEHL, MARÍA CARMEN MARTÍ, YOLANDA VÁSQUEZ: *A degenerating convection-diffusion system modelling froth flotation with drainage*
- 2022-07 RODOLFO ARAYA, CRISTIAN CÁRCAMO, ABNER POZA, EDUARDO VINO: *An adaptive stabilized finite element method for the Stokes-Darcy coupled problem*
- 2022-08 JULIO ARACENA, ADRIEN RICHARD, LILIAN SALINAS: *Synchronizing Boolean networks asynchronously*
- 2022-09 JULIO ARACENA, FLORIAN BRIDOUX, LUIS GOMEZ, LILIAN SALINAS: *Complexity of limit cycles with block-sequential update schedules in conjunctive networks*
- 2022-10 ELIGIO COLMENARES, GABRIEL N. GATICA, JUAN CARLOS ROJAS: *A Banach spaces-based mixed-primal finite element method for the coupling of Brinkman flow and nonlinear transport*
- 2022-11 SERGIO CAUCAO, GABRIEL N. GATICA, RICARDO OYARZÚA, PAULO ZUÑIGA: *A posteriori error analysis of a mixed finite element method for the coupled Brinkman-Forchheimer and double-diffusion equations*
- 2022-12 SERGIO CAUCAO, GABRIEL N. GATICA, JUAN P. ORTEGA: *A posteriori error analysis of a Banach spaces-based fully mixed FEM for double-diffusive convection in a fluid-saturated porous medium*

Para obtener copias de las Pre-Publicaciones, escribir o llamar a: DIRECTOR, CENTRO DE INVESTIGACIÓN EN INGENIERÍA MATEMÁTICA, UNIVERSIDAD DE CONCEPCIÓN, CASILLA 160-C, CONCEPCIÓN, CHILE, TEL.: 41-2661324, o bien, visitar la página web del centro: <http://www.ci2ma.udec.cl>



**CENTRO DE INVESTIGACIÓN EN
INGENIERÍA MATEMÁTICA (CI²MA)
Universidad de Concepción**



Casilla 160-C, Concepción, Chile
Tel.: 56-41-2661324/2661554/2661316
<http://www.ci2ma.udec.cl>